Afdelingen for Bærende Konstruktioner
Department of Structural Engineering
Danmarks Tekniske Universitet • Technical University of Denmark

The HOTCH-POTCH Shell Element - Finite Element for Analysis of Reinforced Concrete Shells

Lars Jagd

Jens Christoffersen

M.P. Nielsen

The HOTCH-POTCH Shell Element - Finite Element for Analysis of Reinforced Concrete Shells

Lars Jagd

Jens Christoffersen

M.P. Nielsen

The HOTCH-POTCH Shell Element - Finite Element for Analysis of Reinforced Concrete Shells

Tryk:
Afdelingen for Bærende Konstruktioner
Danmarks Tekniske Universitet
Lyngby
ISBN 87-7740-154-9
ISSN 0909-587X
Bogbinder:
H. Meyer, Bygning 101, DTU

Abstract

The report describes a new shell element, used for finite element analysis, which is based on simple, mechanical models that cause normal stresses to be concentrated in stringers along the element edges and shear to be transferred by a constant in-plane shear stress field. The torsional and flexural rigidities are separated making independent specifications of these possible.

The element is neither a compatible nor an equilibrium element but is an equilibrium element for a transformed shell consisting of a disk with in-plane rigidity, a plate with no flexural rigidity and a grid system with no torsional rigidity. The element is therefore called the 'Hotch-Potch' shell element or simply the HP shell element.

The element has a behavior very similar to the stringer method and is ideally suited for analyses of e.g. cylindrical shells with stiffeners or reinforced concrete shells.

In the report the geometric stiffness matrix for the element is also developed. This makes it possible to use the element for large deformation analyses.

The element has been implemented in a finite element programme and a number of test problems have been analyzed. Compared with theoretical solutions, all the problems yield very accurate results, the computational efforts taken into account.

Table of Contents

Chapter 1

Introduction

In this report elastic shells are examined for geometrical linear as well as non-linear behavior.

In general, shells are spatially curved structures which resist external loads by a combination of membrane and bending action. Beams and plates primarily have a flexural resistance mechanism while arches, disks and shells primarily have an in-plane resistance mechanism. Generally speaking, loads are resisted much more efficient in in-plane modes rather than in flexural modes. This fact makes the shell structure ideal for a number of applications.

Even for quite simple geometries and material properties few analytical solutions can be found in the literature. Thus shells are most often designed using simplified hand calculation methods or various numerical methods.

Of these numerical methods the finite element methods are by far the most prevalent today. This is due to the fact, that the finite element method is very suitable for implementation in computer programmes. Furthermore the commercial FEM programmes are often coupled to advanced pre- and postprocessors making them very user-friendly.

The significance of FEM programmes for analyses of complicated structures is undisputed. However, it is important to consider the basic assumptions of the programme and the elements used, before the numerical results obtained may be accepted as reasonable approximations to the actual conditions.

In this report a new shell finite element is described. The element is based on simple, mechanical models that cause normal stresses to be concentrated in stringers along the element edges and shear to be transferred by a constant in-plane shear stress field. Furthermore, the torsional and flexural rigidities are

separated making independent specifications of these possible. The element is neither a compatible nor an equilibrium element but is an equilibrium element for a transformed shell consisting of a disk with in-plane rigidity, a plate with no flexural rigidity and a grid-system with no torsional rigidity. The element is therefore called the 'Hotch-Potch' shell element or simply the HP shell element.

Chapter 2

Shell Analysis

2.1 Geometry of Shells

The geometry of a shell is defined by the prescription of the middle surface and the shell thickness in all points. A general C_1 (at least one time differentiable) surface in three dimensional space S is considered, see figure 2.1.

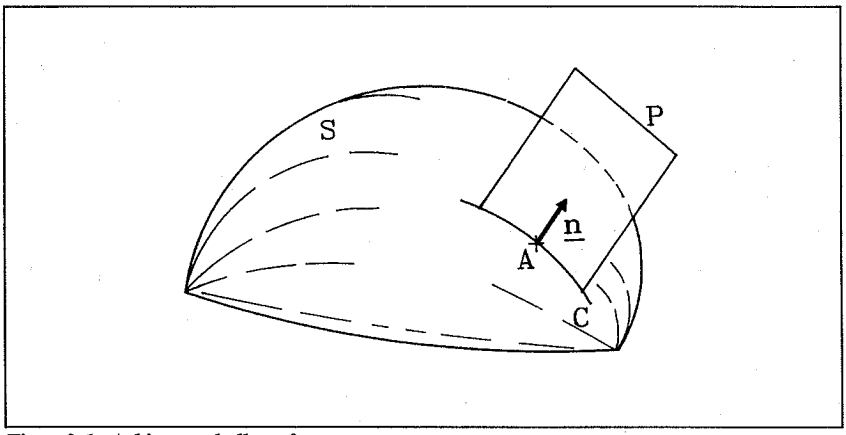

Figur 2.1: Arbitrary shell surface.

In each point A on the surface, a normal vector $\underline{n}$ will exist. An infinite number of planes through A containing $\underline{n}$ exist. The intersection between these planes, e.g. P, and the surface S are plane curves as e.g. the curve C. For each curve, the curvature in A is called κ. The two orthogonal curves containing the

maximum curvature κ_1 and the minimum curvature κ_2 are called the *principal sections* and the curvatures are called the *principal curvatures*.

The product g of the two principal curvatures κ_1 and κ_2 is by definition called the *Gaussian curvature*. On figure 2.2 different types of shell surfaces can be seen.

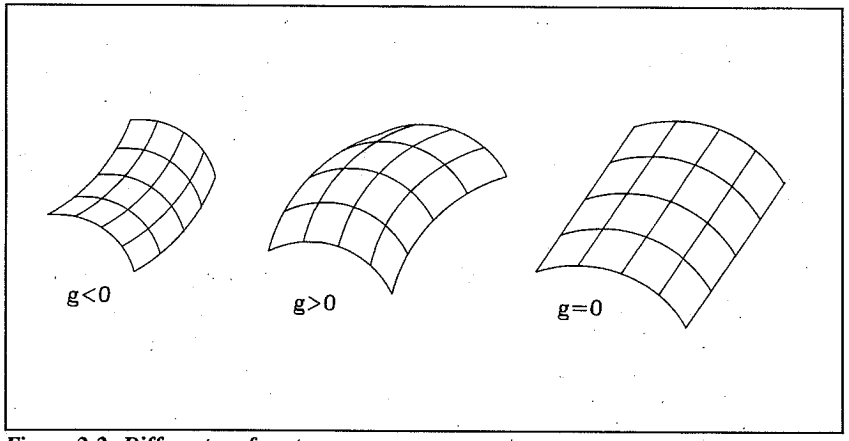

Figure 2.2: Different surface types.

2.2 Internal Forces

On figure 2.3 an infinitesimal element of a shell with general geometry can be seen. The shell curvatures are given by $1/r_x$ and $1/r_y$. The following stresses are present:

1) Normal stresses σ_x and σ_y
2) The transverse shear stresses τ_{xz} and τ_{yz}
3) The in-plane shear stresses τ_{xy} and τ_{yx}

In the design of shell structures most often the stresses are integrated across the shell thickness in order to obtain the shell internal forces, see figure 2.4:

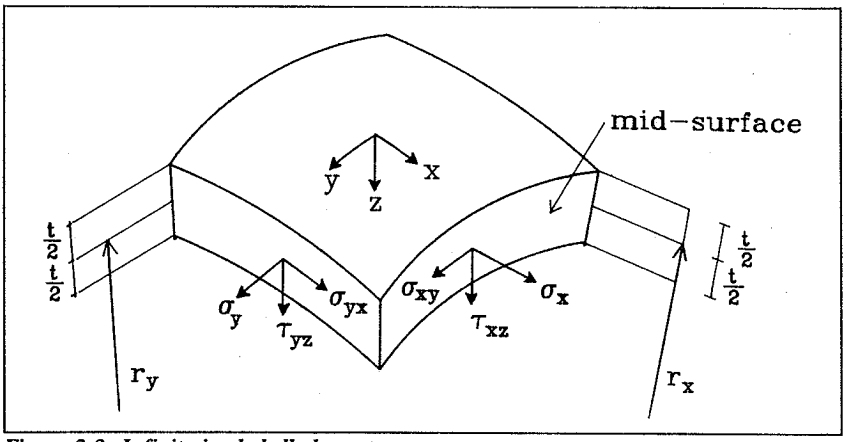

Figure 2.3: Infinitesimal shell element.

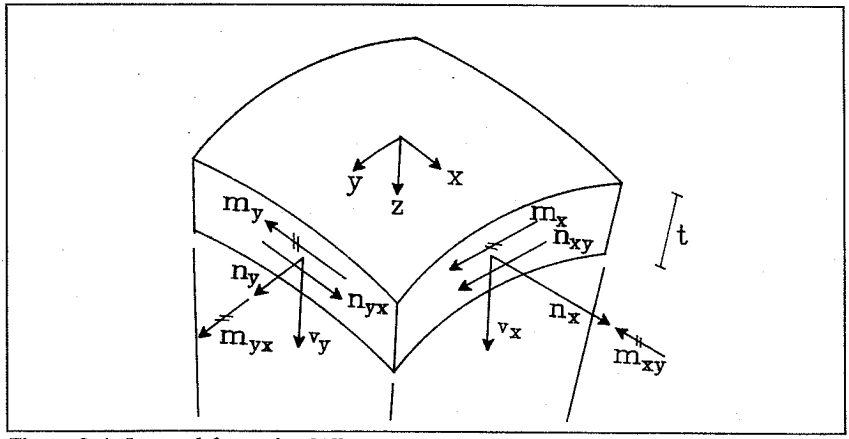

Figure 2.4: Internal forces in shell.

The internal forces can be sub-divided into membrane forces and bending forces. The membrane forces are n_x, n_y, n_{xy} and n_{yx} (N/m), see **(2.1)**. The bending forces are m_x, m_y, m_{xy} (Nm/m), v_x and v_y (N/m), see **(2.2)**.

The z/r-terms in **(2.1-2)** arise because in general the cross section is trapezoidal. When small curvatures are present or when considering plane shells, this term can be neglected.

$$n_x = \int_{-\frac{t}{2}}^{+\frac{t}{2}} \sigma_x \cdot \left(1 + \frac{z}{r_y}\right) dz$$

$$n_y = \int_{-\frac{t}{2}}^{+\frac{t}{2}} \sigma_y \cdot \left(1 + \frac{z}{r_x}\right) dz$$

$$n_{xy} = \int_{-\frac{t}{2}}^{+\frac{t}{2}} \sigma_{xy} \cdot \left(1 + \frac{z}{r_y}\right) dz$$

$$n_{yx} = \int_{-\frac{t}{2}}^{+\frac{t}{2}} \sigma_{yx} \cdot \left(1 + \frac{z}{r_x}\right) dz$$

(2.1)

$$m_x = \int_{-\frac{t}{2}}^{+\frac{t}{2}} z \cdot \sigma_x \left(1 + \frac{z}{r_y}\right) dz$$

$$m_y = \int_{-\frac{t}{2}}^{+\frac{t}{2}} z \cdot \sigma_y \left(1 + \frac{z}{r_x}\right) dz$$

$$m_{xy} = \int_{-\frac{t}{2}}^{+\frac{t}{2}} z \cdot \sigma_{xy} \left(1 + \frac{z}{r_y}\right) dz$$

$$m_{yx} = \int_{-\frac{t}{2}}^{+\frac{t}{2}} z \cdot \sigma_{yx} \left(1 + \frac{z}{r_x}\right) dz$$

(2.2)

$$v_x = \int_{-\frac{t}{2}}^{+\frac{t}{2}} \sigma_{xz} \cdot \left(1 + \frac{z}{r_y}\right) dz$$

$$v_y = \int_{-\frac{t}{2}}^{+\frac{t}{2}} \sigma_{yz} \cdot \left(1 + \frac{z}{r_x}\right) dz$$

For a spatial structure six equilibrium equations are present. As the general shell contains ten force resultants, it is an internally indeterminate structure. In a shell where only membrane forces are present the *membrane theory* of shells can be used. Using a moment equilibrium equation around the normal, it can be concluded that $n_{xy}=n_{yx}$. The two other moment equilibrium equations are identically satisfied. Thus a shell containing only membrane internal forces is statically determinate. When membrane action is prevalent often shells are analyzed and designed using membrane theory. Near supports, concentrated forces and geometric discontinuities bending action is often significant and in such cases bending shell theories must be applied. In the literature a vast number of shell theories may be found. The theories are all founded on sets of *equilibrium, kinematical* and *constitutive* equations accompanied by certain boundary conditions. General shell problems are often very complex and difficult to analyze by hand calculation methods.

2.3 General Remarks

In chapter 3 the stiffness matrix for the HP shell element will be derived analytically. The element is based on simple, mechanical models that cause normal stresses to be concentrated in stringers along the element edges and shear to be transferred by a constant in-plane shear stress field. Furthermore, the torsional and flexural rigidities are separated making independent specifications of these possible.

The following assumptions are valid for the HP shell element:

1) Transverse dimensions are small compared to lateral characteristic dimensions.
2) Normal stresses perpendicular to the shell plane are neglected.
3) Transverse shear strains are neglected.
4) The displacements are small compared to the transverse characteristic dimension. Thus equilibrium may be formulated with respect to the initial undeformed geometry.

These assumptions are used in all classical theories of thin shells and were first stated by *Love*, see ref [44.1].

At the present stage, the HP shell element is rectangular. Thus only shells with zero Gaussian curvature like cylinders or box type surfaces can be analyzed.

In chapter 4 the problem of geometric non-linearity is considered. Due to the often large ratio of curvature to shell thickness in shell structures, stability problems and large deformation behavior is a very important factor in shell analysis.

As the behavior of the HP shell element is very similar to the stringer method, the element is especially suited for analyses of reinforced concrete shells. Applications to reinforced concrete are considered in chapter 5.

Finally, in chapter 6 a number of numerical problems are analyzed.

Chapter 3

The HP Shell Element

3.1 General

A plane shell element can be regarded as a combination of a disk element containing in-plane actions and a plate element containing bending actions. The in-plane actions are uniquely described in terms of the in-plane displacements, u_x and u_y. Similarly the bending actions are uniquely described by the out-of-plane displacement u_z and the rotations about the x- and y axes θ_x and θ_y. For reasons that will be apparent later, the rotation about the z-axis is also taken into account although this displacement does not affect the element stiffness.

Introducing the stiffness matrix $\underline{k}$ and arranging the degrees of freedom for an element with N nodes in the vector $\underline{u}$:

$$\underline{u}^T = (u_x^{i=1}, u_y^{i=1}, u_z^{i=1}, \theta_x^{i=1}, \theta_y^{i=1}, \theta_z^{i=1}, u_x^{i=2}, u_y^{i=2}, \ldots, \theta_y^{i=N}, \theta_z^{i=N}) \qquad (3.1)$$

the relationship between the load vector $\underline{r}$ and $\underline{u}$ can be expressed as

$$\underline{k}\cdot\underline{u} = \underline{r} \qquad (3.2)$$

As there is no relationship between the displacements describing in-plane and bending actions for isotropic, linear elastic shells, the stiffness matrix $\underline{k}$ is found by superimposing the stiffness matrix for in-plane actions $\underline{k}_p$ and the stiffness matrix for bending actions $\underline{k}_b$.

3.2 The HP Shell Element

The HP shell element is a rectangular plane element defined by four nodes, see figure 3.1. The side lengths are l_1 and l_2, resp., and the thickness is t.

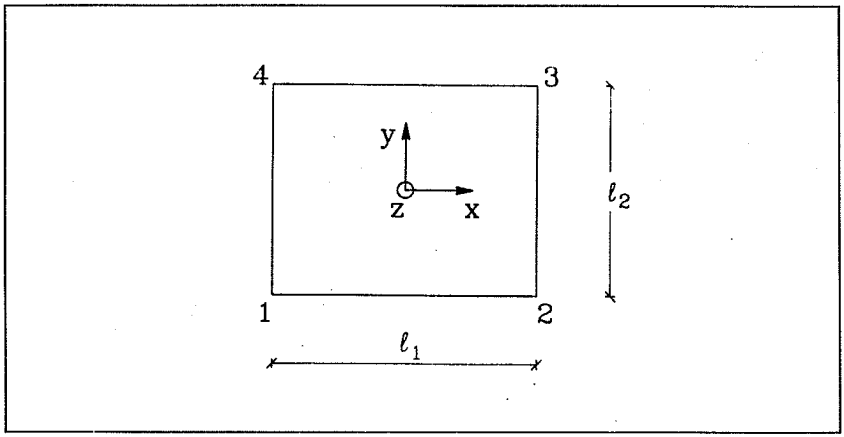

Figure 3.1: The HP Shell Element.

In each node 6 degrees of freedom are present, thus the element contains 24 degrees of freedom, see figure 3.2.

The stiffness contributions from the in-plane actions are taken from the HP disk element, ref [94.1]. This disk element has the following characteristics:

- The element is rectangular and has 4 corner nodes
- The element has 8 degrees of freedom (x- and y-displacements in each node)
- Normal forces are concentrated in stringers along the element edges
- The in-plane shear force is constant within each element
- The side lengths are l_1 and l_2, resp., and the thickness is t

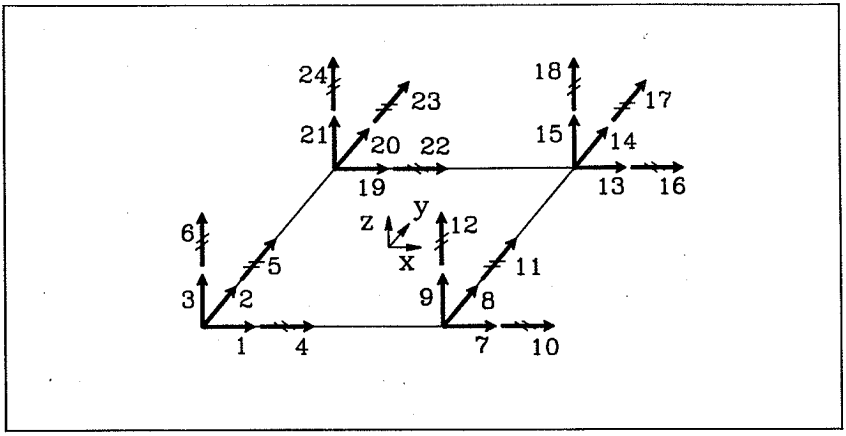

Figure 3.2: Degrees of freedom in the HP shell element.

Arranging the displacements in the vector $\underline{u_p}$:

$$\underline{u_p}^T = (u_x^1 , u_y^1 , u_x^2 , u_y^2 , u_x^3 , u_y^3 , u_x^4 , u_y^4) \tag{3.3}$$

the element stiffness matrix $\underline{k_p}$ is given by:

$$\underline{k} = \begin{bmatrix} k_1+k_5 & k_7 & -k_1+k_5 & -k_7 & -k_5 & -k_7 & -k_5 & k_7 \\ k_7 & k_4+k_6 & k_7 & -k_6 & -k_7 & -k_6 & -k_7 & -k_4+k_6 \\ -k_1+k_5 & k_7 & k_1+k_5 & -k_7 & -k_5 & -k_7 & -k_5 & k_7 \\ -k_7 & -k_6 & -k_7 & k_2+k_6 & k_7 & -k_2+k_6 & k_7 & -k_6 \\ -k_5 & -k_7 & -k_5 & k_7 & k_3+k_5 & k_7 & -k_3+k_5 & -k_7 \\ -k_7 & -k_6 & -k_7 & -k_2+k_6 & k_7 & k_2+k_6 & k_7 & -k_6 \\ -k_5 & -k_7 & -k_5 & k_7 & -k_3+k_5 & k_7 & k_3+k_5 & -k_7 \\ k_7 & -k_4+k_6 & k_7 & -k_6 & -k_7 & -k_6 & -k_7 & k_4+k_6 \end{bmatrix} \tag{3.4}$$

where the constants k_1-k_7 are given by equation **(3.5)**. E is the Young's Modulus and G is the shear modulus.

$$
\begin{aligned}
k_1 &= \frac{1}{2}\cdot E\cdot t\cdot \frac{l_2}{l_1} \\
k_2 &= \frac{1}{2}\cdot E\cdot t\cdot \frac{l_1}{l_1} \\
k_3 &= \frac{1}{2}\cdot E\cdot t\cdot \frac{l_2}{l_1} \\
k_4 &= \frac{1}{2}\cdot E\cdot t\cdot \frac{l_1}{l_2} \\
k_5 &= \frac{1}{4}\cdot G\cdot t\cdot \frac{l_1}{l_2} \\
k_6 &= \frac{1}{4}\cdot G\cdot t\cdot \frac{l_2}{l_1} \\
k_7 &= \frac{1}{4}\cdot G\cdot t
\end{aligned}
\qquad (3.5)
$$

The stiffness contributions from the bending actions $\underline{k}_b$ are taken from the HP plate element, ref [93.1]. Like the HP shell and disk elements the element is rectangular, has 4 corner nodes, side lengths l_1 and l_2 and thickness t. The physical model of the plate element can be described as a plate coupled to a grid system, see figure 3.3.

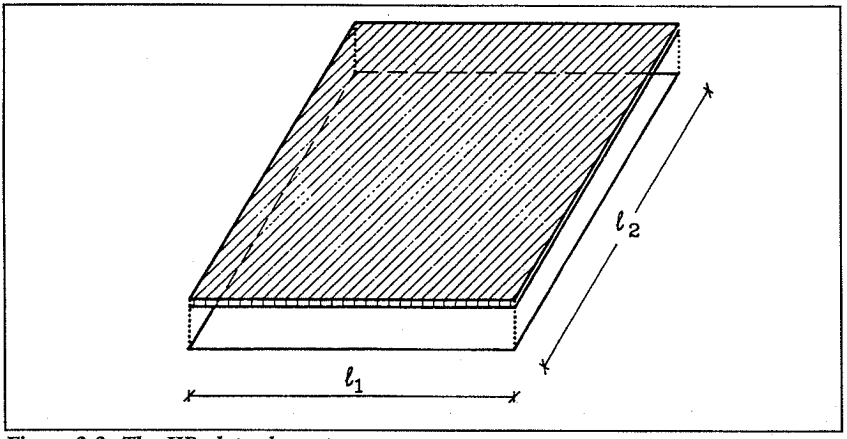

Figure 3.3: The HP plate element.

The grid system consists of four beams connected in four nodes and from each node a connection to the plate is present. The grid system represents flexural stiffness and the plate carries torsional stiffness. The mechanical model is shown on figure 3.4.

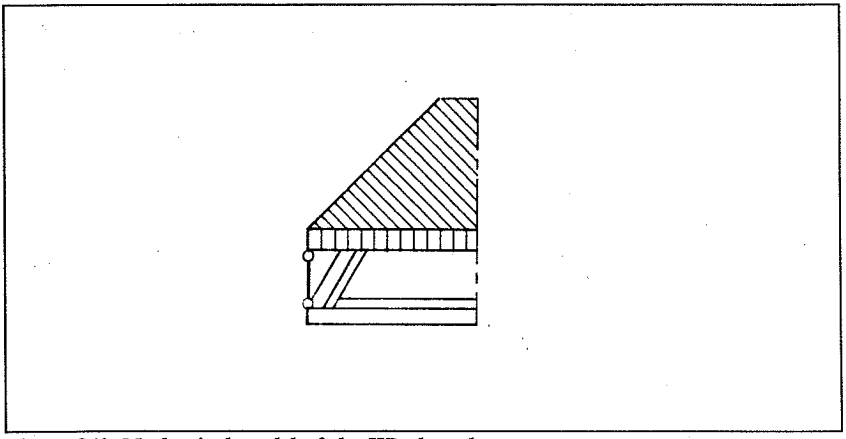

Figure 3.4: Mechanical model of the HP plate element.

It is seen, that the connection between the grid system and the plate can be regarded as a pendulum with hinges in the ends. The length of the pendulum is infinitely small. This mechanical model makes it possible to specify bending and torsional rigidities independently. The element is neither a compatible nor an equilibrium plate element but is an equilibrium element for a transformed plate consisting of a plate with no flexural rigidity and a grid system with no torsional rigidity. The stiffness matrix for the HP plate element $\underline{k}_b$ is given by **(3.6-7)**. I_1 and I_2 are the flexural stiffnesses in the x- and y-direction, resp.

$$\underline{k} = \begin{bmatrix}
c_3+P & c_2 & -c_1 & -c_4-P & 0 & -c_1 & P & 0 & 0 & -c_7-P & c_2 & 0 \\
c_2 & c_5 & 0 & 0 & 0 & 0 & 0 & 0 & 0 & -c_2 & \frac{c_5}{2} & 0 \\
-c_1 & 0 & c_6 & c_1 & 0 & \frac{c_6}{2} & 0 & 0 & 0 & 0 & 0 & 0 \\
-c_4-P & 0 & c_1 & c_3+P & c_2 & c_1 & -c_7-P & c_2 & 0 & P & 0 & 0 \\
0 & 0 & 0 & c_2 & c_5 & 0 & -c_2 & \frac{c_5}{2} & 0 & 0 & 0 & 0 \\
-c_1 & 0 & \frac{c_6}{2} & c_1 & 0 & c_6 & 0 & 0 & 0 & 0 & 0 & 0 \\
P & 0 & 0 & -c_7-P & -c_2 & 0 & c_3+P & -c_2 & c_1 & -c_4-P & 0 & c_1 \\
0 & 0 & 0 & c_2 & \frac{c_5}{2} & 0 & -c_2 & c_5 & 0 & 0 & 0 & 0 \\
0 & 0 & 0 & 0 & 0 & 0 & c_1 & 0 & c_6 & -c_1 & 0 & \frac{c_6}{2} \\
-c_7-P & -c_2 & 0 & P & 0 & 0 & -c_4-P & 0 & -c_1 & c_3+P & -c_2 & -c_1 \\
c_2 & \frac{c_5}{2} & 0 & 0 & 0 & 0 & 0 & 0 & 0 & -c_2 & c_5 & 0 \\
0 & 0 & 0 & 0 & 0 & 0 & c_1 & 0 & \frac{c_6}{2} & -c_1 & 0 & c_6
\end{bmatrix} \tag{3.6}$$

$$
\begin{aligned}
c_1 &= \frac{3 \cdot E \cdot I_1}{l_1^2} \\
c_2 &= \frac{3 \cdot E \cdot I_2}{l_2^2} \\
c_3 &= 6 \cdot E \cdot \left(\frac{I_1}{l_1^3} + \frac{I_2}{l_2^3} \right) \\
c_4 &= \frac{6 \cdot E \cdot I_1}{l_1^3} \\
c_5 &= \frac{2 \cdot E \cdot I_2}{l_2} \\
c_6 &= \frac{2 \cdot E \cdot I_1}{l_1} \\
c_7 &= \frac{6 \cdot E \cdot I_2}{l_2^2} \\
P &= \frac{1}{6} \cdot E \cdot \frac{t^3}{l_1 \cdot l_2}
\end{aligned}
\tag{3.7}
$$

The stiffness matrix for the HP shell element can now be found by combining the stiffness matrixes for the HP disk and the HP plate element, **(3.4)** and **(3.6)**.

$$
\underline{k}_s = \begin{bmatrix}
k_1+k_5 & k_7 & 0 & 0 & 0 & 0 & k_5-k_1 & -k_7 & 0 & 0 & 0 & 0 & -k_5 & -k_7 & 0 & 0 & 0 & 0 & -k_5 & k_7 & 0 & 0 & 0 & 0 \\
 & k_6+k_4 & 0 & 0 & 0 & 0 & k_7 & -k_6 & 0 & 0 & 0 & 0 & -k_7 & -k_6 & 0 & 0 & 0 & 0 & -k_7 & k_6-k_4 & 0 & 0 & 0 & 0 \\
 & & c_3+P & c_2 & -c_1 & 0 & 0 & 0 & -c_4-P & 0 & -c_1 & 0 & 0 & 0 & P & 0 & 0 & 0 & 0 & 0 & -c_7-P & c_2 & 0 & 0 \\
 & & & c_5 & 0 & 0 & 0 & 0 & 0 & 0 & 0 & 0 & 0 & 0 & 0 & 0 & 0 & 0 & 0 & 0 & -c_2 & c_5/2 & 0 & 0 \\
 & & & & c_6 & 0 & 0 & 0 & c_1 & 0 & c_6/2 & 0 & 0 & 0 & 0 & 0 & 0 & 0 & 0 & 0 & 0 & 0 & 0 & 0 \\
 & & & & & 0 & 0 & 0 & 0 & 0 & 0 & 0 & 0 & 0 & 0 & 0 & 0 & 0 & 0 & 0 & 0 & 0 & 0 & 0 \\
 & & & & & & k_5+k_1 & -k_7 & 0 & 0 & 0 & 0 & -k_5 & -k_7 & 0 & 0 & 0 & 0 & -k_5 & k_7 & 0 & 0 & 0 & 0 \\
 & & & & & & & k_2+k_6 & 0 & 0 & 0 & 0 & k_7 & k_6-k_2 & 0 & 0 & 0 & 0 & k_7 & -k_6 & 0 & 0 & 0 & 0 \\
 & & & & & & & & c_3+P & c_2 & c_1 & 0 & 0 & 0 & -c_7-P & c_2 & 0 & 0 & 0 & 0 & P & 0 & 0 & 0 \\
 & & & & & & & & & c_5 & 0 & 0 & 0 & 0 & -c_2 & c_5/2 & 0 & 0 & 0 & 0 & 0 & 0 & 0 & 0 \\
 & & & & & & & & & & c_6 & 0 & 0 & 0 & 0 & 0 & 0 & 0 & 0 & 0 & 0 & 0 & 0 & 0 \\
 & & & & & & & & & & & 0 & 0 & 0 & 0 & 0 & 0 & 0 & 0 & 0 & 0 & 0 & 0 & 0 \\
 & & & & & & & & & & & & k_3+k_5 & k_7 & 0 & 0 & 0 & 0 & k_5-k_3 & -k_7 & 0 & 0 & 0 & 0 \\
 & & & & & & & & & & & & & k_2+k_6 & 0 & 0 & 0 & 0 & k_7 & -k_6 & 0 & 0 & 0 & 0 \\
 & & & & & & & & & & & & & & c_3+P & -c_2 & c_1 & 0 & 0 & 0 & -c_4-P & 0 & c_1 & 0 \\
 & & & & & & & & & & & & & & & c_5 & 0 & 0 & 0 & 0 & 0 & 0 & 0 & 0 \\
 & & & & & & & & & & & & & & & & c_6 & 0 & 0 & 0 & -c_1 & 0 & c_6/2 & 0 \\
 & & & & & & & & & & & & & & & & & 0 & 0 & 0 & 0 & 0 & 0 & 0 \\
 & & & & & & & & & & & & & & & & & & k_3+k_5 & -k_7 & 0 & 0 & 0 & 0 \\
 & & & & & & & & & & & & & & & & & & & k_4+k_6 & 0 & 0 & 0 & 0 \\
 & & & & & & & & & & & & & & & & & & & & c_3+P & -c_2 & -c_1 & 0 \\
 & & & & & & & & & & & & & & & & & & & & & c_5 & 0 & 0 \\
 & & & & & & & & & & & & & & & & & & & & & & c_6 & 0 \\
 & & & & & & & & & & & & & & & & & & & & & & & 0
\end{bmatrix} \qquad \textbf{(3.8)}
$$

Due to the constant in-plane shear force within each element and the fact that bending stiffnesses in two orthogonal directions and torsional stiffness can be specified independently, this new element is ideally suited for analyses of e.g. cylindrical shells with stiffeners or reinforced concrete shells. Applications for reinforced concrete shells are considered in chapter 5.

The element is neither a compatible nor an equilibrium element but is an equilibrium element for a transformed shell consisting of a disk with in-plane rigidity, a plate with no flexural rigidity and a grid system with no torsional rigidity. The element is therefore called the 'Hotch-Potch' shell element or simply the HP shell element.

3.3 Assembly of Elements

Equation **(3.8)** yields the element stiffness matrix in the local element coordinate system. In order to assemble the system stiffness matrix, the element matrices have to be transformed to the global coordinate system and then added together. The method proposed by *Zienkiewicz*, ref. [71.1] section 11.3 is used.

When not all elements joining at a certain node are co-planar, the transformations to global coordinates in such a node require the inclusion of an additional degree of freedom. This is why the rotation θ_z was introduced. However, if all elements joining at a node are co-planar, numerical difficulties will occur as this introduces equations of the form $0=0$ in the governing equations. This problem is solved by introducing an arbitrary stiffness in such nodes. This has no effect on the solution, as θ_z is uncoupled from all the equilibrium equations.

3.4 Sectional Forces

After the displacements have been determined the sectional forces can be calculated. The normal forces and bending moments in each element are found by multiplying the element stiffness matrix by the nodal displacements in the element.

The in-plane shear force is constant in each element and given by, ref [94.1]:

$$n_{xy} = \frac{1}{2} \cdot E_c \cdot t \cdot \phi_{xy} \qquad (3.9)$$

where ϕ_{xy} is the shear strain given by:

$$\phi_{xy} = \frac{u_{13} + u_{19} - u_1 - u_7}{2 \cdot l_2} + \frac{u_8 + u_{14} - u_2 - u_{20}}{2 \cdot l_1} \tag{3.10}$$

The shear force in each stringer is constant and given by **(3.11)**:

$$\begin{aligned} v_x &= \frac{\Delta m_x}{\Delta x} \\ v_y &= \frac{\Delta m_y}{\Delta y} \end{aligned} \tag{3.11}$$

Finally, the torsional moment in each element can be calculated by **(3.12)**, see [93.1]:

$$m_{xy} = -\frac{1}{12} \cdot G \cdot t^3 \cdot \frac{u_9 + u_{21} - u_3 - u_{15}}{l_1 \cdot l_2} \tag{3.12}$$

Chapter 4

Large Deformations of Shells

4.1 General

Structures may under certain loading conditions become unstable for loads of several orders of magnitudes below the loading causing material failure. Especially in the case of shells, the phenomenon of *buckling* is of great significance due to the prevalent in-plane forces and the fact, that shell structures are often very thin compared to the typical dimensions of the structures.

Generally, a body can become unstable in two ways: *Bifurcation of equilibrium* or *Limitation of equilibrium.*

4.1.1 Bifurcation of Equilibrium

In bifurcation of equilibrium a body subjected to increased loading will, at a certain stage, have two possible paths of equilibrium. An example of this behavior is the straight elastic column subjected to axial loading. In the beginning the axial shortening is proportional to the applied load, see figure 4.1.

At a certain load P_{cr}, the well-known Euler load, the path splits into two, as now two states of equilibrium are possible. In reality the structure choses the path that yields the minimum elastic energy of the system. The point at which the load path bifurcates is called the *bifurcation point* and the corresponding load is called the *stability load.*

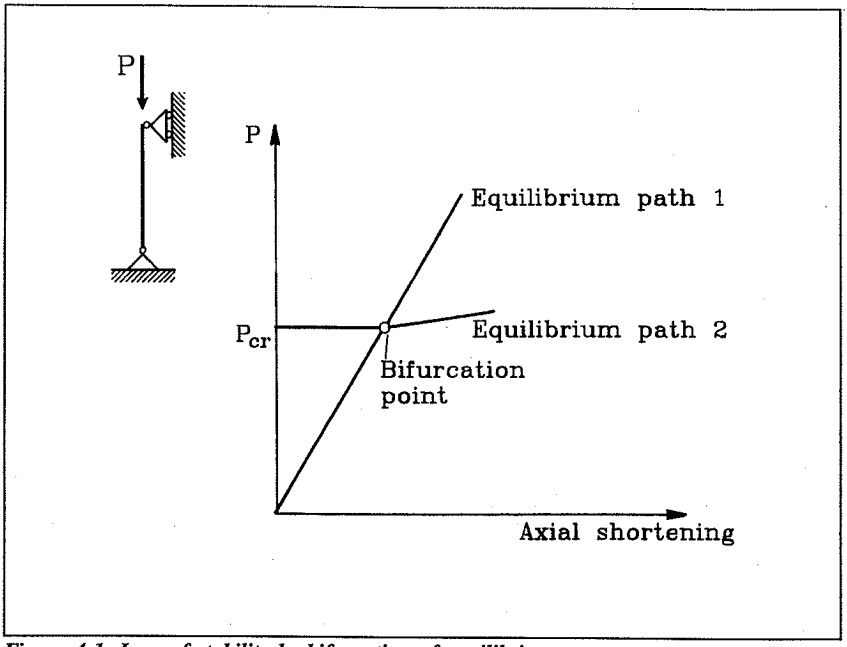

Figure 4.1: Loss of stability by bifurcation of equilibrium.

4.1.2 Limitation of Equilibrium

Loss of stability by limitation of equilibrium is characteristic for structures which carry the transverse loading mainly by compressive axial forces. The load/deformation path is continuous with certain maximum and minimum points. The stability load corresponds to one of these points. An example of a structural system with this behavior can be found in the so-called *snap-through* problem, see figure 4.2.

In the following sections solution methods for the HP shell element for both types of stability loss are developed.

4.2 The Initial Stability Problem

The general finite element formulation of an incremental large displacement problem is of the following form, ref [71.1], section 19.2.

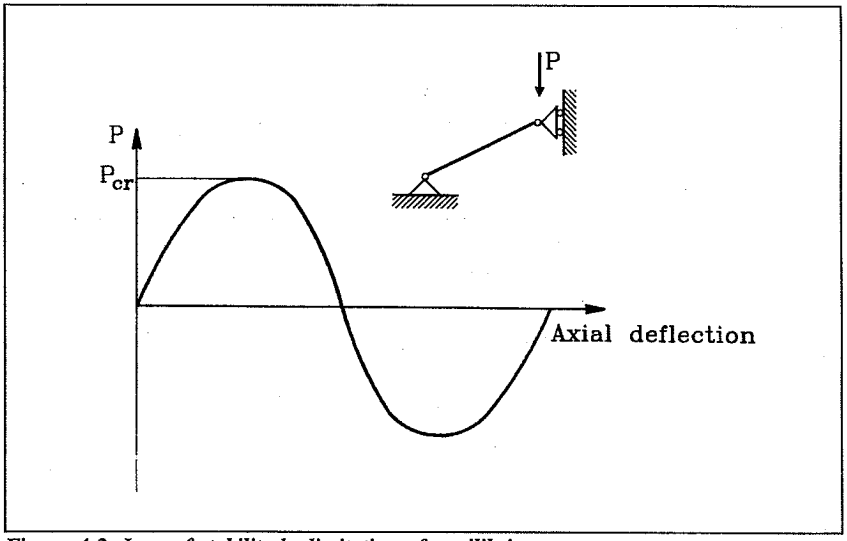

Figure 4.2: Loss of stability by limitation of equilibrium.

$$\left(\underline{K} - \underline{K}_g - \underline{K}_L\right)\cdot \underline{du} = \underline{dR} \qquad (4.1)$$

$\underline{K}$ is the *stiffness* matrix, $\underline{K}_g$ the *geometric stiffness* matrix and $\underline{K}_L$ the *large displacement* matrix. The geometric stiffness matrix contains forces corresponding to the additional loads which the in-plane stresses cause due to out-of-plane deformations. The large deformation matrix represents the non-linear effects of the strain/displacement relationship which occur in a large displacement problem.

In order to determine the stability load in an elastic bifurcation problem, an eigenvalue problem, the so-called *initial stability* problem, occurs, ref [71.1] section 19.2.

$$\left(\underline{K} - \lambda\cdot \underline{K}_g\right)\cdot \underline{u} \equiv \underline{0} \qquad (4.2)$$

This formulation is only valid when the deformations found in the static solution cause all components of the large deformation matrix to be zero. This is the case in problems of the type seen in figure 4.1.

The geometric stiffness matrix $\underline{k}_g$ for the HP shell element will now be derived. Contributions are present from the in-plane nodal forces.

On figure 4.3 stringer 1-2 is considered.

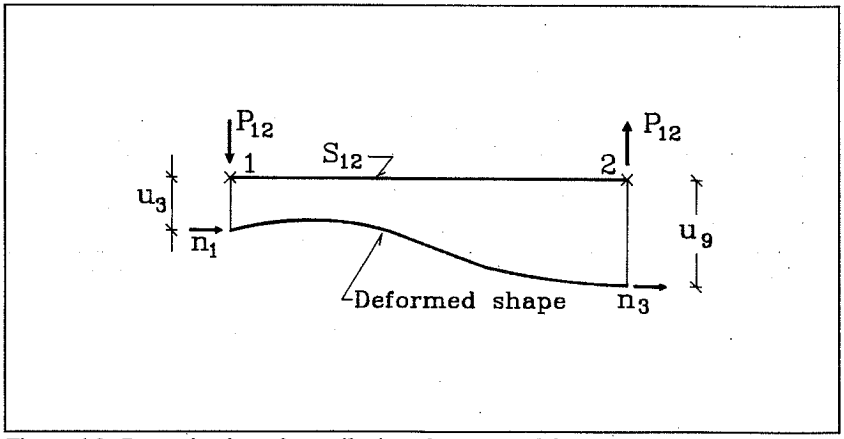

Figure 4.3: Determination of contributions from normal forces.

The normal forces in node 1 and 2 are referred to as n_1 and n_3, resp. The mean normal stress in the stringer, n_{12}, causes a moment about the y-axis which equals the difference in transversal displacements between node 1 and 2 multiplied by the normal force. This moment is equivalent to the moment caused by the vertical forces P_{12} on figure 4.3, see equation **(4.3)**.

$$P_{12} = \frac{1}{2} \cdot n_{12} \cdot \frac{l_2}{l_1} \cdot (u_9 - u_3) \tag{4.3}$$

Similarly, the vertical forces P_{23}, P_{34} and P_{41} due to the normal forces in the other three stringers are given by:

$$\begin{aligned} P_{23} &= \frac{1}{2} \cdot n_{23} \cdot \frac{l_1}{l_2} \cdot (u_{15} - u_9) \\ P_{34} &= \frac{1}{2} \cdot n_{34} \cdot \frac{l_2}{l_1} \cdot (u_{21} - u_{15}) \\ P_{41} &= \frac{1}{2} \cdot n_{41} \cdot \frac{l_1}{l_2} \cdot (u_3 - u_{21}) \end{aligned} \tag{4.4}$$

The geometric stiffness matrix for the HP shell element can now be formulated. In equation **(4.5)** all non-zero components of $\underline{k}_g$ can be seen:

$$
\begin{aligned}
&k_g(3,3) = K_1 + K_4 \\
&k_g(9,9) = K_1 + K_2 \\
&k_g(15,15) = K_2 + K_3 \\
&k_g(21,21) = K_3 + K_4 \\
&\\
&k_g(3,9) = k_g(9,3) = -K_1 \\
&k_g(3,21) = k_g(21,3) = -K_4 \\
&k_g(9,15) = k_g(15,9) = -K_2 \\
&k_g(15,21) = k_g(21,15) = -K_3
\end{aligned}
\qquad \textbf{(4.5)}
$$

The values of K_1-K_4 are given by **(4.6)**:

$$
\begin{aligned}
K_1 &= \frac{1}{2} \cdot n_{12} \cdot \frac{l_2}{l_1} \\
K_2 &= \frac{1}{2} \cdot n_{23} \cdot \frac{l_1}{l_2} \\
K_3 &= \frac{1}{2} \cdot n_{34} \cdot \frac{l_2}{l_1} \\
K_4 &= \frac{1}{2} \cdot n_{41} \cdot \frac{l_1}{l_2}
\end{aligned}
\qquad \textbf{(4.6)}
$$

In order to solve the general *initial stability* problem, the following calculation process is adapted:

1) Load is applied
2) Linear finite element calculation is performed
3) Normal forces and in-plane shear forces are calculated
4) Geometric stiffness matrix is calculated
5) The eigenvalue problem is solved using Lanczo iteration

In most cases only the lowest load factor will be of interest. The Lanczo method is capable of calculating any number of eigenvalues from the lowest and upwards (up to the number of degrees of freedom in the system).

4.3 General non-linear deformation Path

As mentioned, the solution method described in the previous section can only be used for problems where the large deformation matrix $\underline{K}_L$ is identically zero. When this is not the case, the entire load/deformation path must be followed using a load incrementation method.

In order to determine the path from zero to a given value, either loads or deformations are prescribed stepwise and the increments in deformations/loads are found. For each step equation **(4.1)** must be solved. However, the effect of the matrix $\underline{K}_L$ can alternatively be obtained by in each step adjusting the nodal coordinates in the calculation of the stiffness matrix. Thus **(4.1)** is reduced to **(4.7)**:

$$\left(\underline{K} - \underline{K}_g\right) \cdot \underline{du} = \underline{dR} \qquad \textbf{(4.7)}$$

The stresses must be known in order to find $\underline{K}_g$. These can be found in two ways:

1) The stresses are adjusted incrementaly so that in each step the increments in stresses due to the increment in deformations are added to the stress state in the previous step.
2) In each step the stresses are calculated directly from the strains. This is possible by using Green's strain tensor which yields valid strains whether the deformations are small or large.

As the geometric stiffness matrix depends on the stresses and these depend on the deformations in the step that is being solved, equation **(4.7)** must be solved by an iterative process. The following solution method has been used in order to determine the load/deformation path for a general elastic geometrically non-linear shell problem using the HP shell element.

1) Load increment is applied
2) Stiffness matrix is determined from present nodal coordinates
3) Displacement increments are determined by LU-factorization and back-substitution

4) The total stresses are determined by adding the stress increments of the present load step to the total stresses at the last load step or directly from the total displacements using Green's tensor
5) Geometric stiffness matrix is determined from total stresses and present nodal coordinates
6) Stiffness matrix is corrected by subtracting geometric stiffness matrix
7) New displacements increments are determined by LU-factorization and back-substitution
8) Difference between old and new displacement increments is calculated. If the difference is larger than a user-specified value go to 5) using new displacements
9) Correct nodal coordinates are found by adding displacements, go to 1).

Chapter 5

Applications to Reinforced Concrete

In the following chapter, the HP Shell Element will be developed specifically for calculation of reinforced concrete structures in the serviceability limit state. This involves introduction of relevant material parameters as well as the inclusion of additional iterative steps in the solution methods described in the previous chapter.

5.1 Introduction of relevant Material Parameters

5.1.1 Disk Behavior

For description of the disk behavior, the following material parameters are used:

1) The reinforcement ratios ρ in each direction
2) Young's Modulus for steel E_s
3) Young's Modulus for concrete E_c
4) The shell thickness t
5) The shear modulus for concrete G_c

The normal stiffness for each stringer depends on whether the stress-state in the stringer is tensile or compressive. The constants k_1-k_4 in **(3.5)** are therefore given by one of two possible expressions of the following type **(5.1)**:

$$k = \frac{1}{2} \cdot E_s \cdot \rho \cdot \frac{l_2}{l_1} \vee k = \frac{1}{2} \cdot E_c \cdot t \cdot \frac{l_2}{l_1} \qquad \textbf{(5.1)}$$

An iterative process has to be applied in order to determine the correct stiffnesses, see section 5.2.

5.1.2 Plate Behavior

The following material parameters are used for describing the plate behavior:

1) The reinforcement ratios ρ in top and bottom in each direction
2) Young's Modulus for steel E_s
3) Young's Modulus for concrete E_c
4) The shell thickness t
5) The effective depths h_{ef} of all reinforcement layers

The bending stiffness D for a cracked reinforced concrete section can be calculated by **(5.2)**, see ref. [93.1].

$$D = \frac{1}{2}\cdot E_c \cdot \beta^2 \cdot \left(1 - \frac{1}{3}\cdot\beta\right)\cdot h_e^3$$
$$\beta = \frac{E_s}{E_c}\cdot\rho\cdot\left(\sqrt{1 + \frac{2}{n\cdot\rho}} - 1\right) \qquad (5.2)$$

The stiffnesses can be calculated independently for each stringer and then used in the expressions for c_1-c_7 in **(3.7)**.

The torsional stiffness D_{xy} of an isotropically reinforced concrete slab is calculated by the following expression, see ref. [93.1].

$$D_{xy} = \frac{1}{4}\cdot k_1^2 \cdot \left(1 - \frac{2}{3}\cdot k_1\right)\cdot E_c \cdot t^3$$
$$k_1 = 2\cdot k_2 \cdot \left(\sqrt{1 + \frac{1}{2\cdot k_2}} - 1\right) \qquad (5.3)$$
$$k_2 = \rho\cdot\frac{E_s}{E_c}$$

This expression is used in the calculation of P in equation **(3.7)**.

Generally, the flexural stiffness of each stringer depends on the sign of the bending moment at this position. Therefore and iterative process has to be used.

5.2 Changes in the Solution Method

As the normal and bending stiffnesses depend on the sign of the normal stresses and bending moments resp., additional iterative procedures have to be introduced in the solution method, see sections **5.2.1** and **5.2.2**.

5.2.1 Linear Static Analysis

The signs of the normal stresses and bending moments are assumed. From these assumptions the element stiffness matrixes are calculated and the deformations are found. It is then checked whether the assumptions are correct. If just one fails, a new calculation is performed according to the actual stress states in the previous calculation. The iterative process stops when all assumptions have been found correct or after a given number of iterations specified by the user.

5.2.2 Geometrically non-linear Analyses

In an initial stability problem first the linear static calculation is performed as described in section 5.2.1. On the basis of the sectional forces the geometric stiffness matrix is calculated and the stability loads are found by the eigenvalue technique described in section 4.2.

In the general geometric non-linear problem, iteration procedures as described in section 5.2.1 have to be performed in each load step. In order to reduce the calculation time, as an approximation, the stress-states in the previous load step can be used to determine $\underline{K}_g$.

Chapter 6

Numerical Examples

In order to test the performance of the element, the HP Shell element will be used for analyses of a number of different problems. These are:

1) Linear analysis of a cylindrical vault
2) Linear analysis of liquid retaining cylindrical shell
3) Stability load of a rectangular disk
4) Stability load of a bridge arch
5) Stability load of an axially loaded perfect cylinder
6) Snap-through problem
7) Stability load of a cylinder with imperfections

6.1 Linear Analysis of a Cylindrical Vault

On figure 6.1 a circular cylindrical roof with radius r loaded by its weight p is shown.

In order to analyze this problem a cylinder coordinate system is used. Figure 6.2 shows an infinitesimal section of a circular cylindrical shell and the quantities necessary for fomulating the membrane and bending equilibrium equations.

The membrane force functions are, see ref. [92.1]:

$$\begin{aligned} n_\theta &= r p_z \\ n_{x\theta} &= -\int \left(p_\theta + \frac{1}{r} \frac{\partial n_\theta}{\partial \theta} \right) dx + f_1(\theta) \\ n_x &= -\int \left(p_x + \frac{1}{r} \frac{\partial n_{x\theta}}{\partial \theta} \right) dx + f_2(\theta) \end{aligned} \qquad \textbf{(6.1)}$$

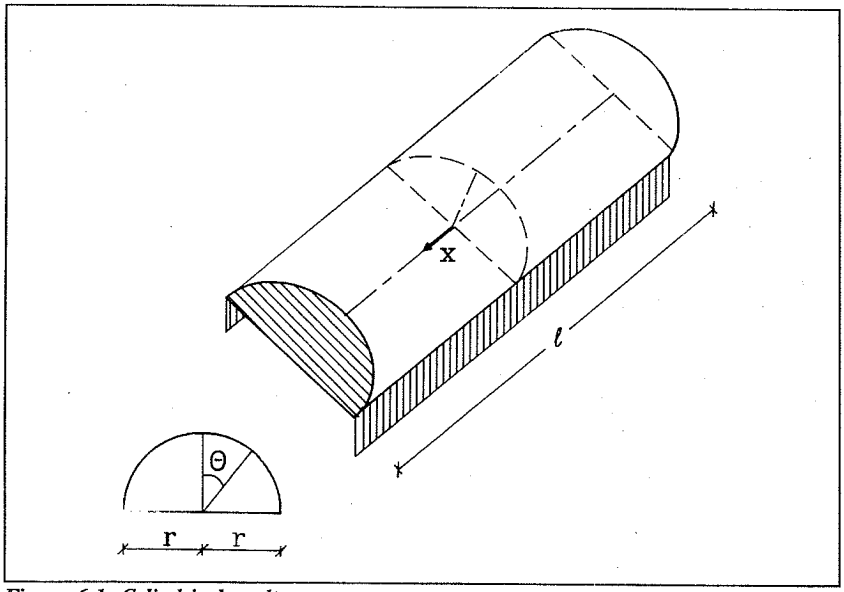

Figure 6.1: Cylindrical vault.

The functions f_1 and f_2 depend on the boundary conditions of the particular problem.

In the two ends the roof is supported by diaphragms which are able to resist in-plane deformations but unable to resist out-of-plane deformations. The roof is also supported in the four corners and on the longitudinal edges in the x-direction. Thus shear force $n_{x\theta}$ can be transferred here. Apart from the areas near the diaphragms where some bending will occur, the displacement field in such a structure will be pure membrane. Thus the problem is suited for analyzing the membrane behavior of the HP shell element.

The components of the weight loading are:

$$\begin{aligned} p_\theta &= p \cdot \sin\theta \\ p_z &= -p \cdot \cos\theta \end{aligned} \qquad \textbf{(6.2)}$$

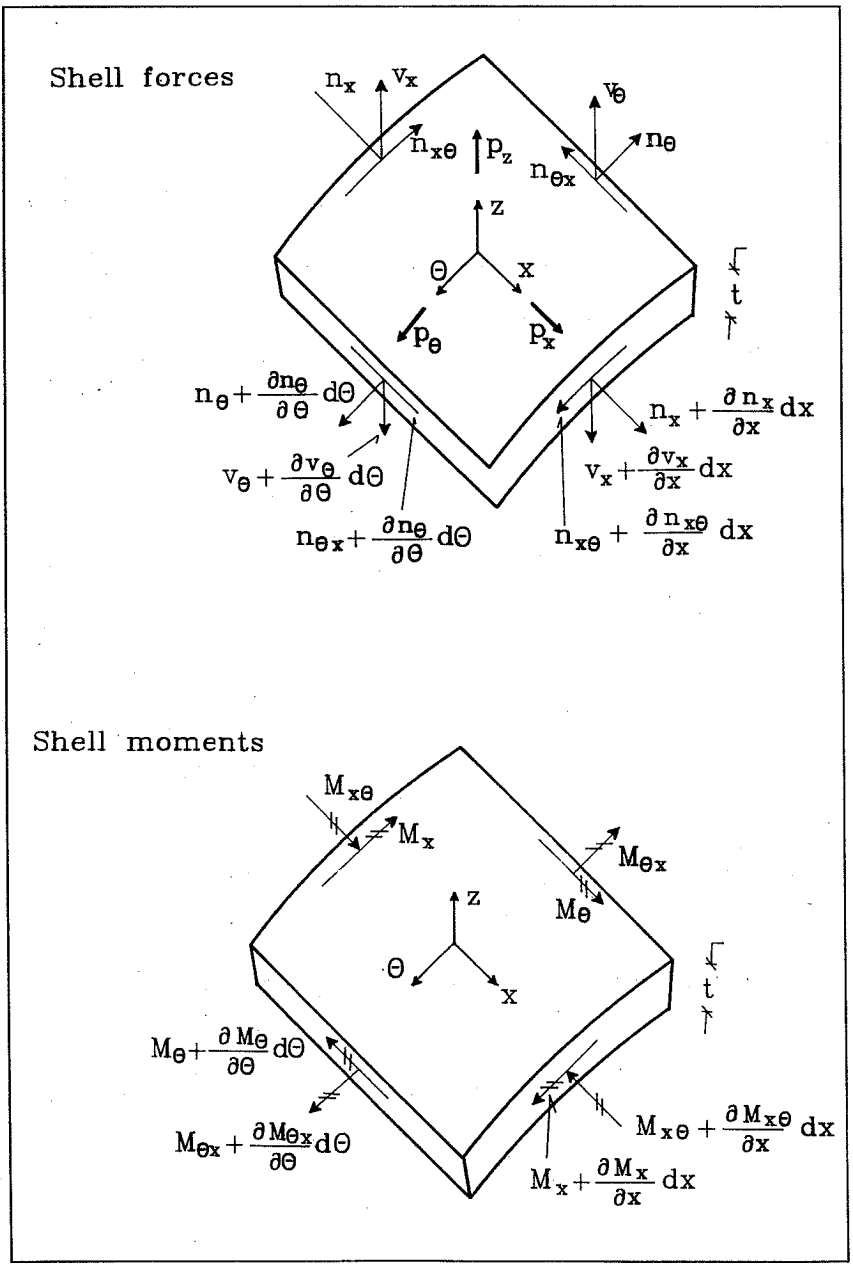

Figure 6.2: Infinitesimal element of circular, cylindrical shell.

As $n_x=0$ in the ends, **(6.1)** reduces to:

$$\begin{aligned} n_\theta &= -p\cdot r\cdot\cos\theta \\ n_{x\theta} &= -2\cdot p\cdot x\cdot\sin\theta \\ n_x &= -\frac{p}{4\cdot r}\cdot(l^2 - 4\cdot x^2)\cdot\cos\theta \end{aligned} \tag{6.3}$$

Assuming Poisson's ratio $\nu=0$ and combining the constitutive and kinematic relations for a linear elastic, isotropic circular cylindrical shell, the following relations are obtained:

$$\begin{aligned} \epsilon_x &= \frac{1}{E\cdot t}\cdot n_x = \frac{\partial u}{\partial x} \\ \epsilon_\theta &= \frac{1}{E\cdot t}\cdot n_\theta = \frac{1}{r}\cdot\left(\frac{\partial v}{\partial\theta} + w\right) \\ \phi_{x\theta} &= \frac{2}{E\cdot t}\cdot n_{x\theta} = \frac{\partial v}{\partial x} + \frac{1}{r}\cdot\frac{\partial u}{\partial\theta} \end{aligned} \tag{6.4}$$

Here u is the longitudinal displacement, v the tangential displacement and w the transverse displacement.

Combining **(6.3-4)**, the deformations (u,v,w) can be found, see equation **(6.5)**.

$$\begin{aligned} u &= \frac{p\cdot x}{E\cdot t\cdot r}\cdot\left(\frac{x^2}{3} - \frac{1}{4}\cdot l^2\right)\cdot\cos\theta \\ v &= \frac{p}{8\cdot E\cdot t}\cdot(l^2 - 4\cdot x^2)\cdot\left(\frac{5\cdot l^2 - 4\cdot x^2}{24\cdot r^2} + 4\right)\cdot\sin\theta \\ w &= -\frac{p}{8\cdot E\cdot t}\cdot(l^2 - 4\cdot x^2)\cdot\left(\frac{5\cdot l^2 - 4\cdot x^2}{24\cdot r^2} + 4\right)\cdot\cos\theta - \frac{p\cdot r^2}{E\cdot t}\cdot\cos\theta \end{aligned} \tag{6.5}$$

A FEM-calculation has been made with the following data:

- Young's Modulus $E=1$
- Shell thickness $t=0.25$
- Length of roof $l=40$
- Radius $r=10$

- Due to symmetry only one half of the structure has been modelled (one quarter of a cylinder). Finite element meshes of *(10x10)* and *(15x15)* have been used.

On figures **(6.3-5)**, *w*- and *u*-displacements at $\theta=0$ and v-displacements at $\theta=\pi/2$ found by **(6.5)** and by the HP shell element, resp., are compared. The agreement is seen to be good.

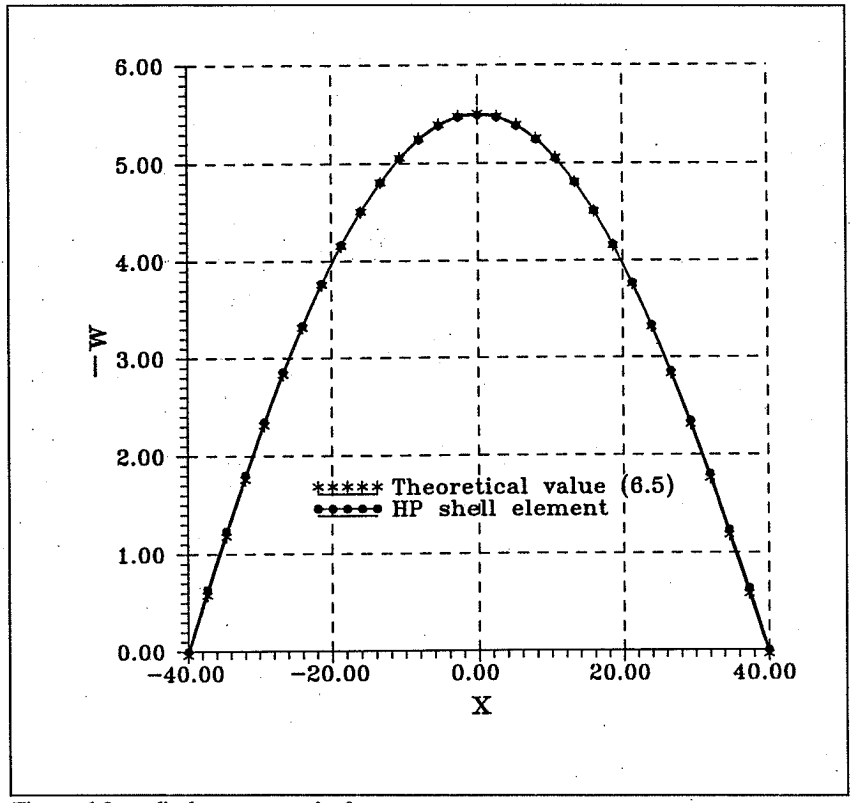

Figure 6.3: w-displacements at $\theta=0$.

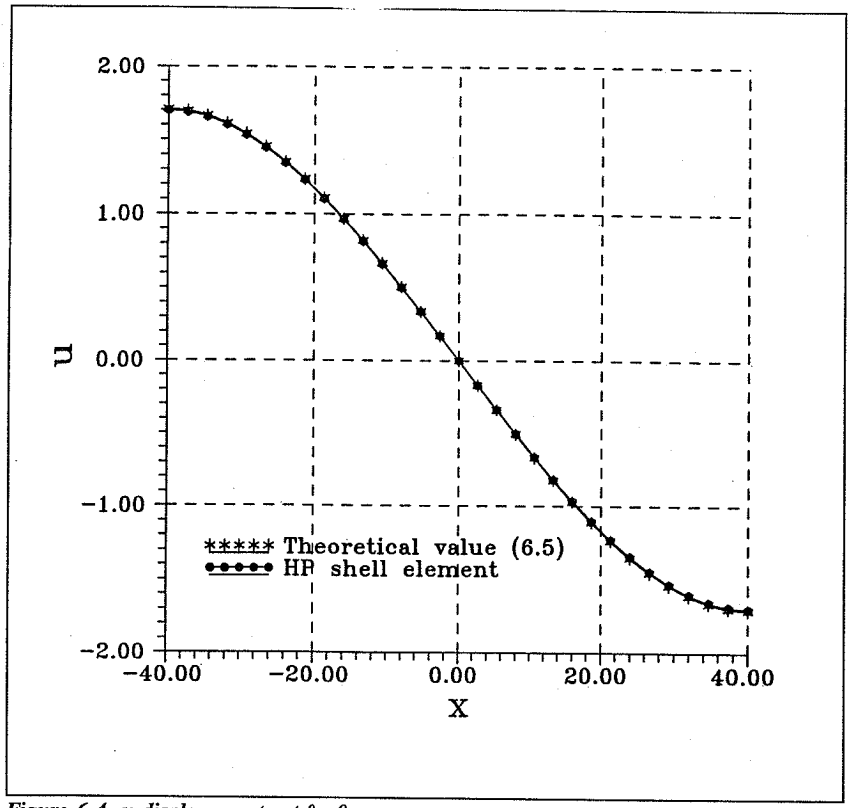

Figure 6.4: u-displacements at $\theta=0$.

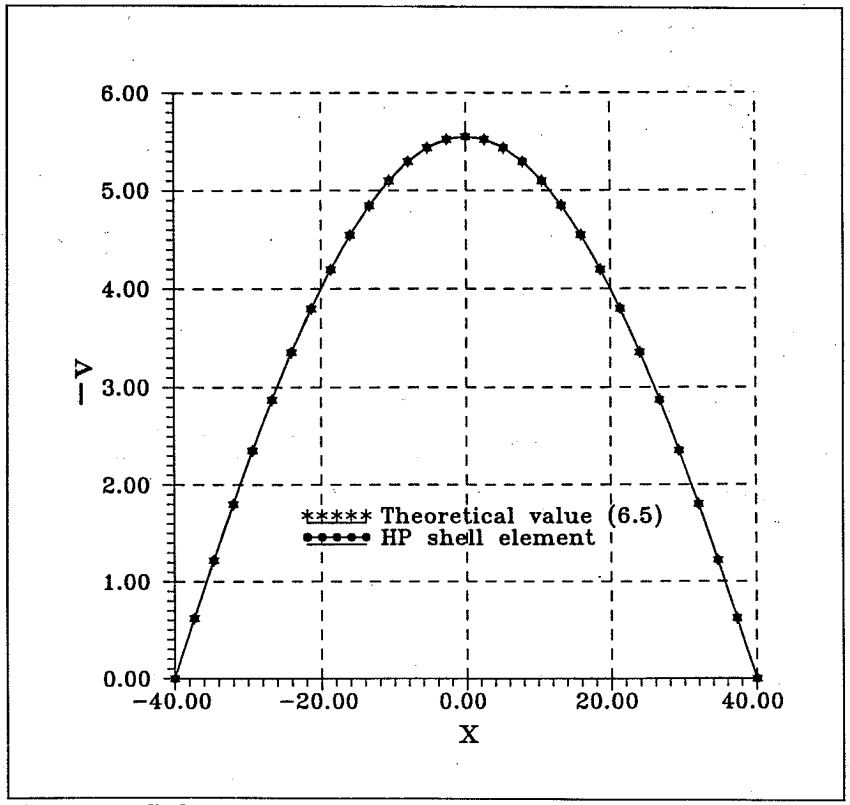

Figure 6.5: **v-*displacements at* $\theta=\pi/2$.**

6.2 Linear Analysis of a Liquid Retaining Cylindrical Shell

A liquid retaining cylindrical shell is examined, see figure 6.6.

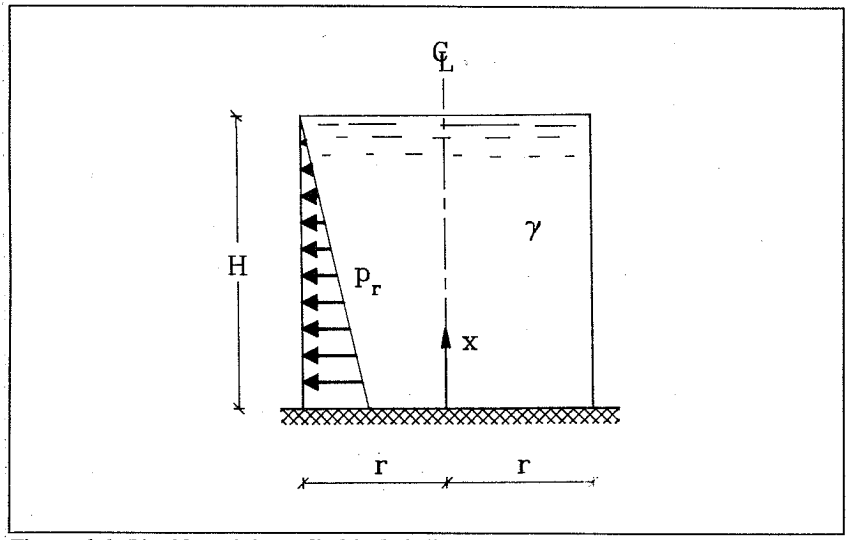

Figure 6.6: Liquid retaining cylindrical shell.

The pressure from the liquid with unit weight γ is given by **(6.6)**:

$$p_r = \gamma \cdot (H - x) \tag{6.6}$$

The following governing differential equation is assumed, see ref. [92.1]:

$$\frac{E \cdot t^3}{12} \cdot (1 - \nu^2) \cdot \frac{d^4 w}{dx^4} + \frac{E \cdot t}{r^2} \cdot w = p_r \tag{6.7}$$

E is Young's Modulus, t is the shell thickness, ν is Poisson's ratio and w is the transverse displacement.

Combining **(6.6)** and **(6.7)** the following general solution for the transverse displacement w is obtained, see ref [92.1]:

$$w = e^{\beta \cdot x}\left(c_1 \cdot \cos(\beta \cdot x) + c_2 \cdot \sin(\beta \cdot x)\right) + e^{-\beta \cdot x}\left(c_3 \cdot \cos(\beta \cdot x) + c_4 \cdot \sin(\beta \cdot x)\right) + \frac{\gamma \cdot (H-x) \cdot r^2}{E \cdot t} \tag{6.8}$$

where:

$$\beta = \left(\frac{3 \cdot (1-\nu^2)}{r^2 \cdot H^2}\right)^{\frac{1}{4}} \tag{6.9}$$

Assuming that the container is so high, that the constraints at the base will not be felt at the top, we may set $c_1 = c_2 = 0$. Furthermore, using the edge conditions **(6.10)** at the base:

$$\begin{aligned} w &= 0 \ , \quad for \ x = 0 \\ \frac{dw}{dx} &= 0 \ , \quad for \ x = 0 \end{aligned} \tag{6.10}$$

the following solution for the radial displacement is obtained **(6.11)**:

$$w = \frac{\gamma \cdot r^2}{E \cdot t} \cdot \left[H - x - e^{-\beta \cdot x} \cdot \left(H \cdot \cos(\beta \cdot x) + (H - \frac{1}{\beta}) \cdot \sin(\beta \cdot x)\right)\right] \tag{6.11}$$

The hoop stress n_θ and the bending moment m_x of the cylinder, see figure 6.2, can be derived from **(6.11)**:

$$\begin{aligned} n_\theta &= \gamma \cdot r \cdot \left[H - x - H \cdot e^{-\beta \cdot x} \cdot \cos(\beta \cdot x) + (\frac{1}{\beta} - H) \cdot e^{-\beta \cdot x} \cdot \sin(\beta \cdot x)\right] \\ m_x &= -\frac{\gamma \cdot r \cdot t}{\sqrt{12 \cdot (1 - \nu^2)}} \cdot \left[(\frac{1}{\beta} - H) \cdot e^{-\beta \cdot x} \cdot \cos(\beta \cdot x) + H \cdot e^{-\beta \cdot x} \cdot \sin(\beta \cdot x)\right] \end{aligned} \tag{6.12}$$

A FEM-calculation has been made with the following data:

- Young's Modulus $E=1$
- Poisson's ratio $\nu=0$
- Shell thickness $t=0.25$
- Unit weight of liquid $\gamma=10$
- Height of container $H=40$, radius $r=10$
- Due to symmetry only one quarter of the cylinder has been modelled.

For determining the hoop-stresses, a finite element mesh of *(10,15)* in the θ- and x-direction, resp., has been used. All elements have the same size.

In figure 6.7 the results for the hoop stresses obtained by the HP shell element are compared to **(6.12)**. The agreement is seen to be fine.

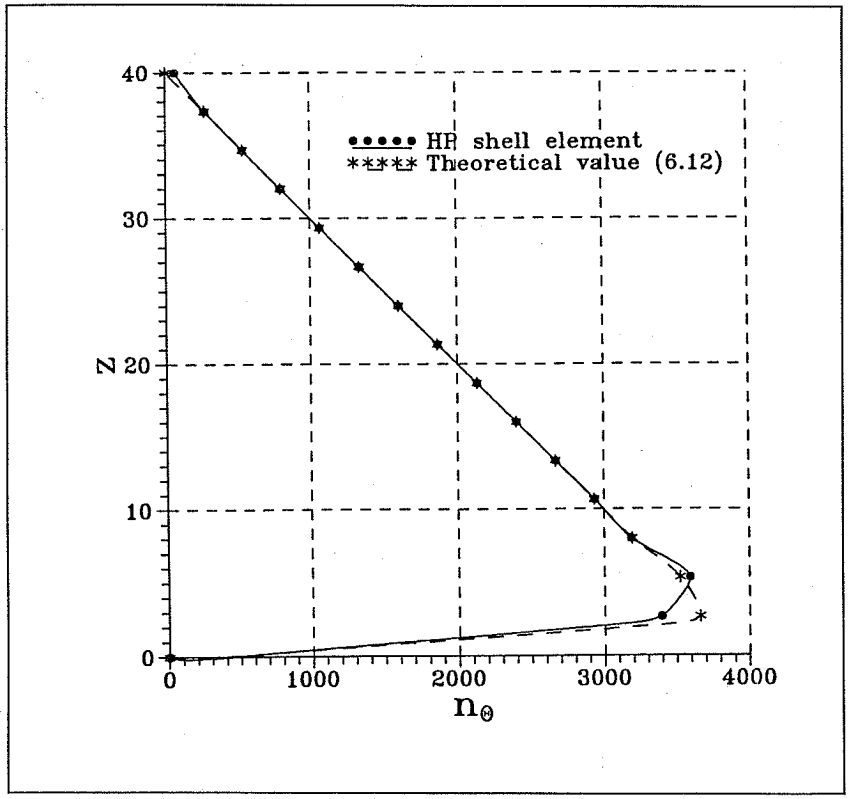

Figure 6.7: Comparison of hoop stresses.

For determining the bending moments m_x the same number of elements has been used, but the size in the x-direction has been varied so that the elements near the base are smaller, see figure 6.8.

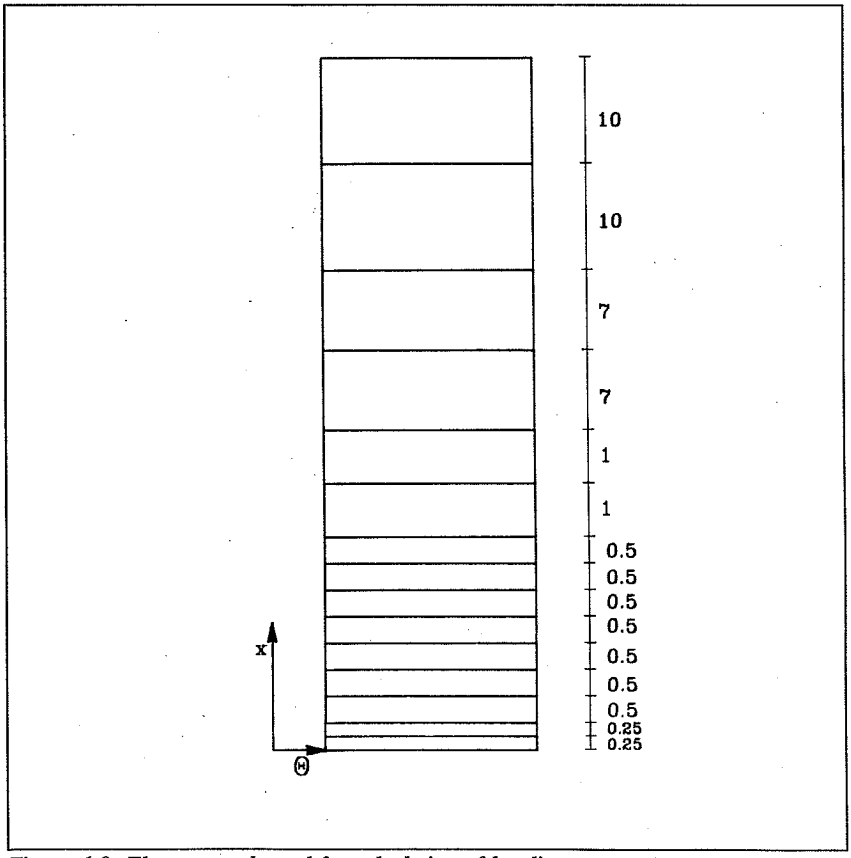

Figure 6.8: Element mesh used for calculation of bending moments.

In figure 6.9a and 6.9b the results for the bending moments m_x obtained by the HP shell element are compared to **(6.12)**. The agreement is again seen to be good.

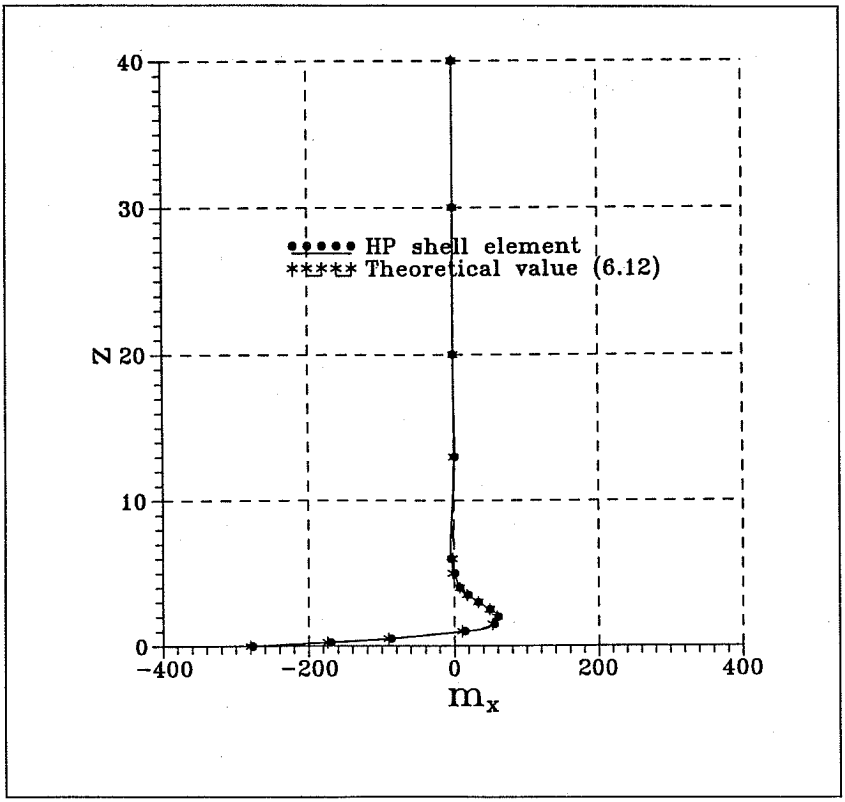

Figure 6.9a: Comparison of results for bending moments.

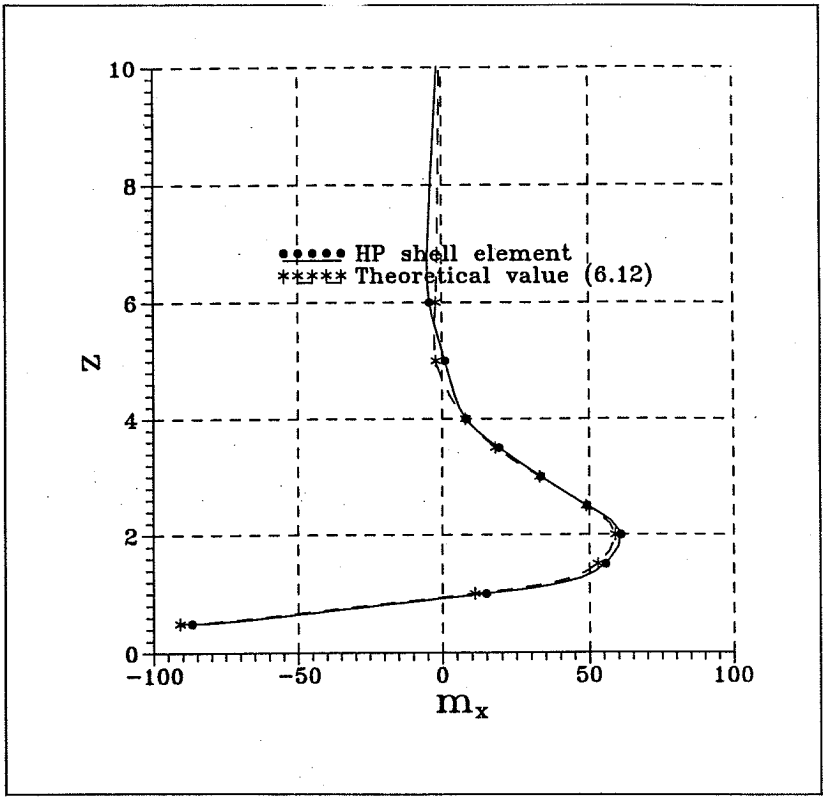

Figure 6.9b: Comparison of results for bending moments (detail of figure 6.9a).

6.3 Stability Load of a Rectangular Disk

The stability load of a plane, rectangular disk, see figure 6.10, is determined.

- The in-plane dimensions *(a,b)* are *(8,8)*
- The disk thickness $t=1$
- Young's Modulus $E=1$
- The line load $p=1$
- An element mesh of *(4x8)* HP shell elements is used

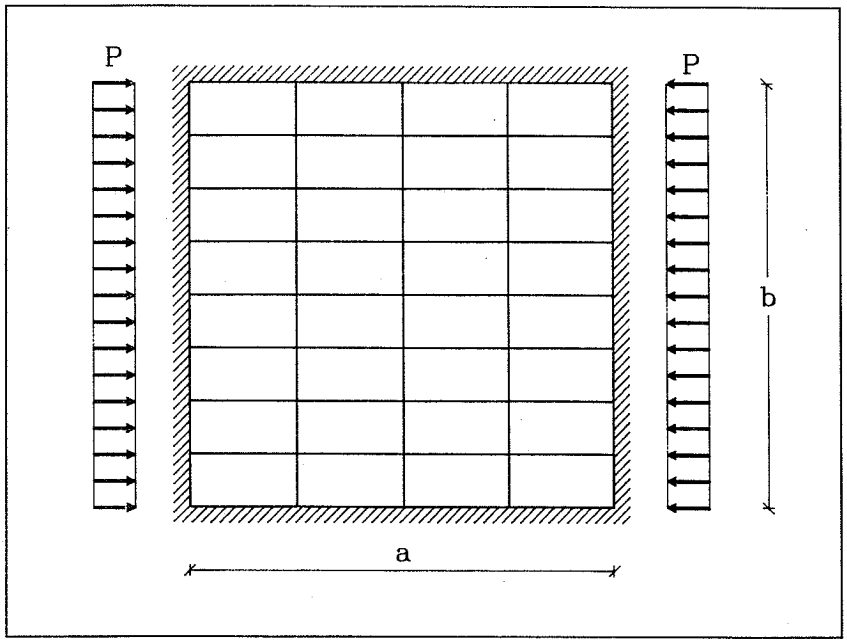

Figure 6.10: Stability load of rectangular disk.

The structure looses its stability by bifurcation. The large deformation matrix is identically zero until the disk buckles. Thus the buckling load is found by an eigenvalue calculation as described in section 4.2.

The critical load σ_{cr} is found to be 0.050534. The theoretical value found in ref. [61.1] is 0.051404, corresponding to an error of 1.9%.

6.4 Stability Load of a Bridge Arch

The stability load for the arch structure seen in figure 6.11 is determined. For low arches the internal forces in the structure are primarily in-plane and only small bending moments are present. Thus the large deformation matrix can be assumed identically zero, and an eigenvalue analysis is performed in order to determine the stability load.

In ref [45.1] *Engelund* determines the stability load for a bridge arch as a function of the arch length b and the radius of the arch r, see **(6.13)**. The normal force is assumed constant.

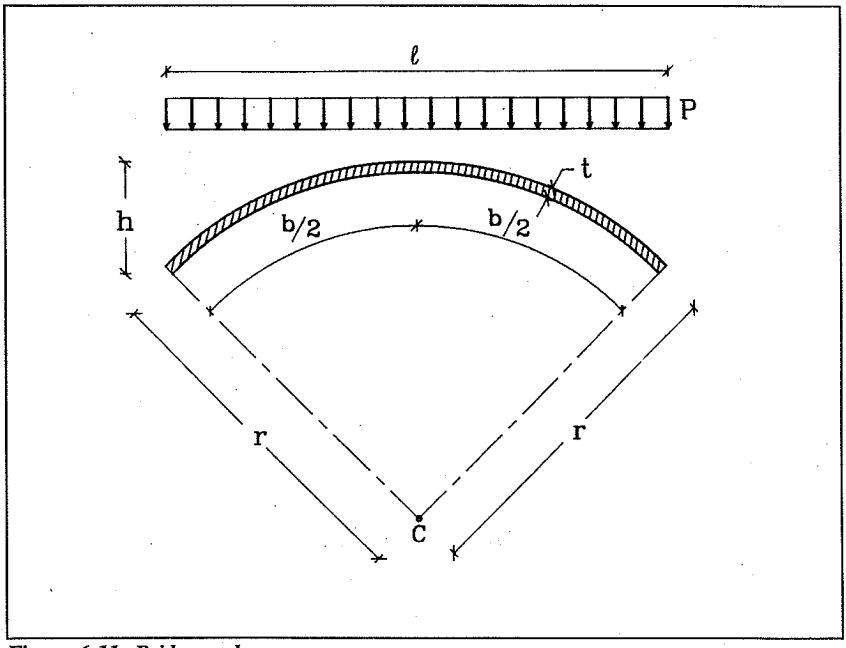

Figure 6.11: Bridge arch.

$$N_E = \left(\frac{4 \cdot \pi^2}{b^2} - \frac{1}{r^2}\right) \cdot E \cdot I \qquad \textbf{(6.13)}$$

E is the Young's Modulus and I the moment of inertia of the bridge section.

If the term $1/r^2$ is neglected, equation **(6.14)** is obtained. This is seen to be similar to the Euler load for a straight elastic column subject to axial loading.

$$N_E = \frac{\pi^2 \cdot E \cdot I}{\left(\frac{b}{2}\right)^2} \qquad \textbf{(6.14)}$$

The problem in figure 6.11 has been analyzed with the following parameters:

- The dimensions *(l,h)* are *(√50,10√50)*
- The width of the arch is *10*
- The shell thickness $t=1$

- Young's Modulus $E=1$
- The line load $p=2$
- An element mesh of *(1x8)* HP shell elements is used

The variation in normal force along the arch is found to be $n=16.45\text{-}20.64$ and the critical load factor is found to be $\lambda=0.00743043$. Thus the variation in the normal force at the critical load is $n=0.1222\text{-}0.1534$.

The theoretical critical load found by **(6.13)** is $n=0.125$. As expected, this is seen to be almost similar to the lowest normal force found in the FEM-calculation.

The buckling mode is identical to the buckling mode of an straight elastic column subject to axial loading.

6.5 Stability Load of an Axially Loaded Perfect Cylinder

An axially loaded perfect cylinder is analyzed with respect to buckling, see figure 6.12.

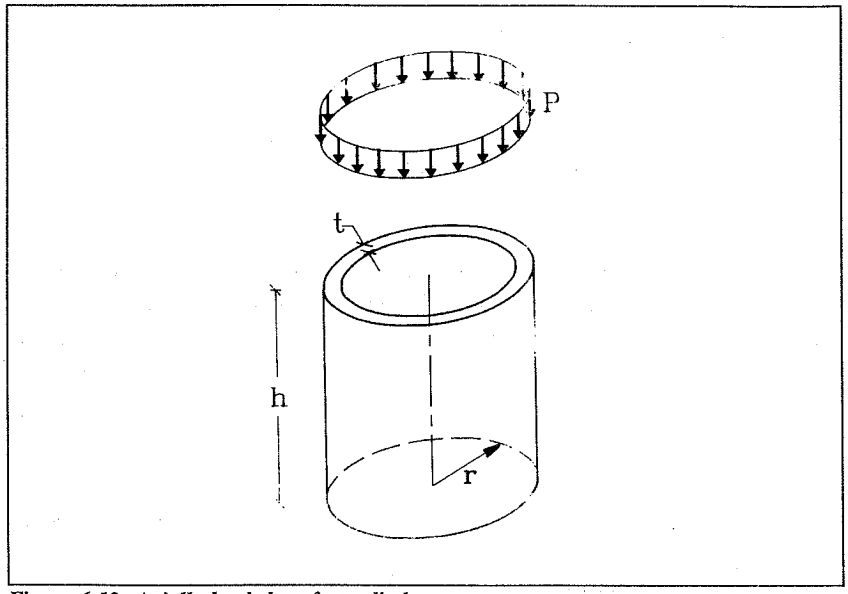

Figure 6.12: Axially loaded perfect cylinder.

Assuming that the cylinder is long, that the shell thickness is small and that a symmetrical sinus buckling form occurs, the critical stress of a perfect cylinder is according to ref. [61.1] given by **(6.15)**

$$\sigma_{cr} = \frac{E \cdot t}{\sqrt{3 \cdot (1-\nu^2)}} \qquad \textbf{(6.15)}$$

The length of one wave is given by **(6.16)**:

$$l = 2 \cdot \pi \cdot \left(\frac{r^2 \cdot t^2}{12 \cdot (1-\nu^2)} \right)^4 \qquad \textbf{(6.16)}$$

A cylinder with the following characteristics is analyzed:

- The dimensions *(r,h)* are *(20,21.3508)*.
- The shell thickness $t=2$.
- Young's Modulus $E=1$.
- Due to symmetry only one quarter of the cylinder is modelled. An element mesh of *(8x16)* HP shell elements is used.

The height $H=21.3508$ corresponds to one wavelength according to **(6.16)**. The theoretical critical stress according to **(6.15)** is $\sigma_{cr}=0.057735$. The result from the FEM analysis is $\sigma_{cr}=0.058671$ which corresponds to an error of 1.6%.

6.6 Snap-through Problem

The beam on figure 6.13 is loaded by the force P. The beam cross-section area is A, the initial position is given by z and the displacement by w. The initial length of the beam is l and in the deformed state the length is l'.

The structure looses its stability by limitation of equilibrium and is an example of a snap-through problem, se section 4.1.2. The problem will be examined in order to check the behavior of the HP shell element for such a problem.

By vertical equilibrium the relation between P and the normal force N is given by **(6.17)**:

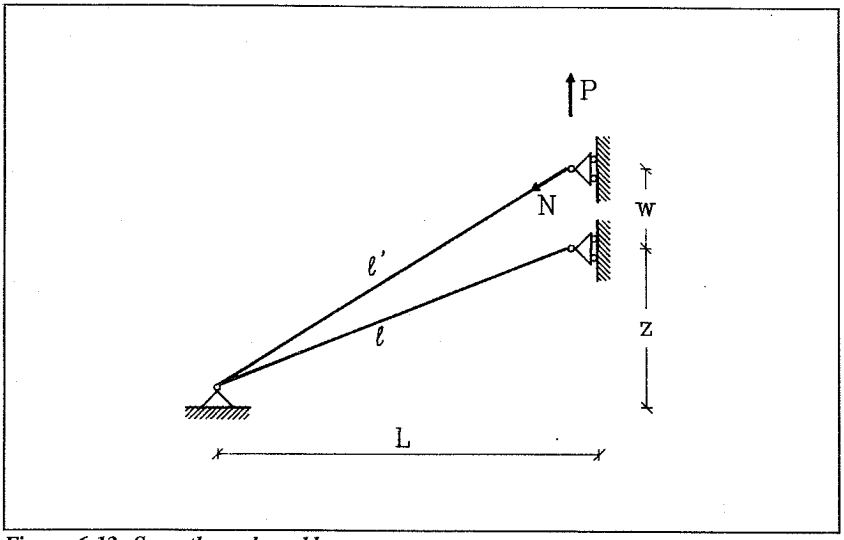

Figure 6.13: Snap-through problem.

$$P = N \cdot \frac{z+w}{l'} \approx \frac{z+w}{l} \tag{6.17}$$

The normal strain ϵ is approximately given by **(6.18)**:

$$\epsilon \approx \frac{z}{l} \cdot \frac{w}{l} \cdot + \frac{1}{2} \cdot \left(\frac{w}{l}\right)^2 \tag{6.18}$$

Assuming the material to be linear elastic, the normal force N can be found as:

$$N = \epsilon \cdot E \cdot A \tag{6.19}$$

By combining **(6.17-19)**, the following relation between the force P and the displacement w is obtained.

$$P = \frac{E \cdot A}{l^3} \cdot \left(w \cdot z^2 + \frac{3}{2} \cdot z \cdot w^2 + \frac{1}{2} \cdot w^3 \right) \qquad (6.20)$$

The problem has been calculated using the following data:

- The dimensions *(L,z)* are *(8,8/10)*
- The shell thickness $t=1$
- The width of the beam is $y=10$
- Young's Modulus $E=1$
- An element mesh of *(2x8)* HP shell elements is used
- Stresses are calculated incrementally
- Load is applied as incrementally prescribed displacements up to $w=8/10$

On figure 6.14 the results obtained for $N=10$, $N=20$ *and* $N=40$ load steps, resp., are compared to the theoretical result **(6.20)**. It is seen, that the maximum load is predicted quite accurately using even the large load steps.

If the rotation terms in **(6.18)** are neglected, the following load/displacement path is obtained **(6.21)**:

$$P = \frac{E \cdot A}{l^3} \cdot \left(z^2 \cdot w + z \cdot w^2 \right) \qquad (6.21)$$

The significance of the rotation terms in **(6.18)** is quite important. The maximum value of **(6.21)** is almost 30% too large. This clearly demonstrates the effect of the large deformation matrix, see equation **(4.1)**.

6.7 Stability Load of a Cylinder with Imperfections

Determining the stability load of thin steel cylinders has been the subject of many investigations. Generally it is observed, that even very small imperfections result in much lower stability loads than the theoretical values for perfect cylinders. The stability loads of test-specimens are typically below 50% of the theoretical values.

In 1933 *Lundquist* and *Donell* made an extensive series of tests on thin cylindrical shells, ref [61.1] pp. 468. None of the test specimens showed a stability load above 60% of the theoretical value. Furthermore, in these tests it

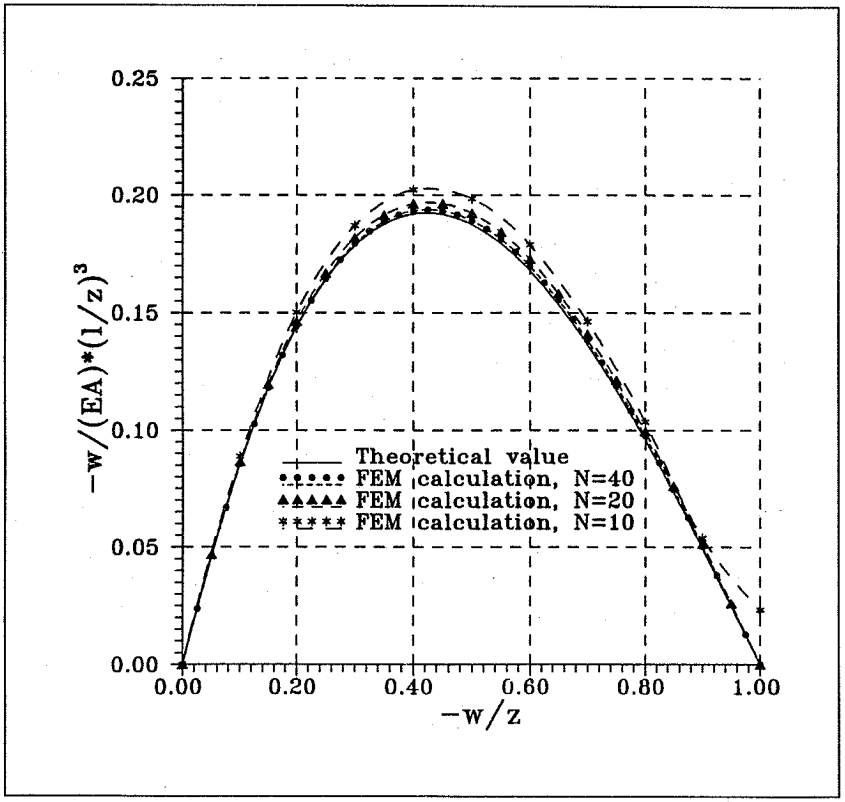

Figure 6.14: Results for three different number of load steps compared to (6.20).

was found that the stability load decreases slightly with increased ratio between the radius r and the shell thickness t. This was explained as being due to the bending which occurs on account of the inevitable initial deformations and a theory accounting for this behavior was developed.

Another important contribution within this field was given by *Kármán*, ref. [41.1]. *Kármán* assumed that the conditions of equilibrium between the stresses acting in the middle surface of a thin shell can approximately be expressed by the equations for flat plates. Introducing *Airy's* stress function F, substituting the large strain compability equations and the elastic stress/strain equations into F and assuming a function of the radial displacements, the total strain energy of the buckled shell can be obtained. The energy of the external compressive force is then calculated, and the parameters in the assumed function for the radial

displacements can be calculated by minimizing the total energy of the system.

The behavior of the HP shell element has been tested by determining stability loads for cylinders with different imperfections. The following problem has been examined:

- The dimensions $(h,r)=(4.27016,20)$, see figure **6.12**. The height h corresponds to the length of one wave according to **(6.16)**.
- The shell thickness $t=0.08$, thus the r/t-ratio is 250
- Young's Modulus $E=1$
- An element mesh of $(16x8)$ in the (x,θ)-directions, resp., is used
- Stresses are calculated incrementaly
- Imperfections have been applied in the form of one sinus-wave with ratios between the amplitudes d and the shell thickness t of ½, 1, 2 and 3, resp.

On figure 6.15 the results of the FEM analysis are compared with the results obtained by *Kármán* and *Koiter*, ref[73.1]. These results have been taken from [79.1]. P^0_{cr} is the stability load of a perfect cylinder. The results from the FEM calculation are seen to be between the two sets of theoretical results.

The effect of different r/t-ratios has also been examined. If has been found, that different ratios yield the same results as in figure 6.15.

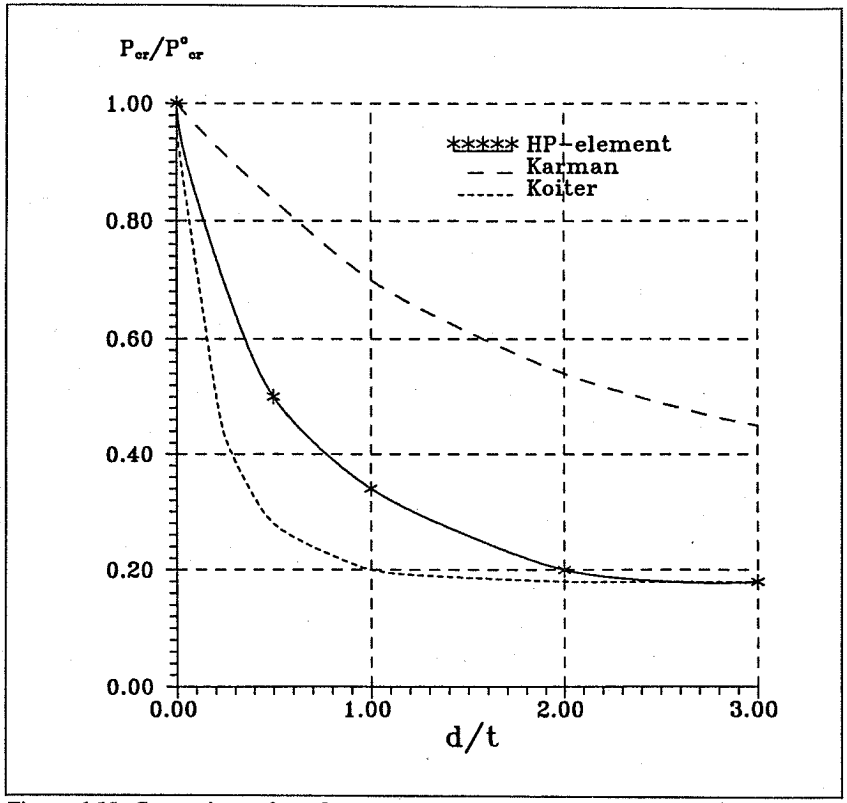

Figure 6.15: Comparison of results.

Chapter 7

Conclusion

In this report a new FEM shell element called the Hotch-Potch shell element has been developed. The element is neither a compatible nor an equilibrium element but is an equilibrium element for a transformed shell consisting of a disk with in-plane rigidity, a plate with no flexural rigidity and a grid system with no torsional rigidity. The element is based on a simple, mechanical model that makes it possible to specify bending stiffnesses in two orthogonal directions and torsional stiffness independently. Similar to the stringer method, the element has a constant in-plane shear force. The element is ideally suited for analyses of e.g. cylindrical shells with stiffenners or reinforced concrete shells.

In the report the geometric stiffness matrix for the element is also developed. This makes it possible to use the element for large deformation analyses.

The stiffness and geometric stiffness matrices have been derived analytically so that numerical integration is avoided.

The element has been implemented in a FEM programme. The programme is capable of performing static and eigenvalue analyses as well as general large deformation analyses by a load increment method. The user may specify bending stiffnesses in two orthogonal directions, the shell thickness and Young's Modulus. The results consist of deformations, reactions, bending moments, torsional moments, out-of-plane shear forces, in-plane shear forces and normal forces. Sectional forces are given for each element separately and as node mean forces. In eigenvalue analysis the user may specify the number of eigenvalues to be calculated and the maximum number of iteration vectors that should be used in Lanczo's method. The results consist of the critical load factors and the displacement modes. In large deformation analyses, the user may specify the number of load steps and results may be obtained for each step.

The programme has been used for calculating a number of numerical examples. The membrane and bending behavior of the element has been tested, analyses have been performed on a flat plate, a bridge arch and a perfect cylinder. The non-linear load/deformation path of a snap-through problem has been determined and the influence of different sizes of initial imperfections in circular cylinders with respect to stability load has been analyzed. All the examples yield very accurate results, the computational efforts taken into account.

Notation

b : Arch length
d : Amplitude
D : Bending stiffness
E : Young's Modulus
E_c : Young's Modulus of the concrete
E_s : Young's Modulus of the steel
F : Airy's stress function
G : Shear modulus
G_c : Shear modulus of the concrete
h : Arch height
H : Height
I : Moment of inertia
I_1 : Moment of inertia in x-direction
I_2 : Moment of inertia in y-direction
$\underline{k}$: Element stiffness matrix
$\underline{k}_g$: Element geometric stiffness matrix
$\underline{k}_p$: Stiffness matrix for in-plane actions
$\underline{k}_b$: Stiffness matrix for bending actions
$\underline{K}$: System stiffness matrix
$\underline{K}_g$: System geometric stiffness matrix
$\underline{K}_L$: System large displacement matrix
l : Length
l' : Length in deformed state
l_1 : Side length
l_2 : Side length
m_x : Bending moment about y-axis
m_{xy} : Torsional moment in xy-plane
m_y : Bending moment about x-axis
n_x : Normal force in x-direction
n_y : Normal force in y-direction
n_{xy} : Shear force in xy-plane
N_E : Euler load

p : Force
p_x : Force in x-direction
p_z : Force in z-direction
p_θ : Force in θ-direction
P : Concentrated force
P_{cr} : Euler load
$\underline{r}$: Element load vector
$\underline{R}$: System load vector
t : Thickness
$\underline{u}$: Displacement vector
$\underline{u}_p$: In-plane displacement vector
u : Longitudinal displacement
u_x : Displacement in x-direction
u_y : Displacement in y-direction
u_z : Displacement in z-direction
v : Tangential displacement
v_x : Shear force in yz-plane
v_y : Shear force in xz-plane
w : Transverse displacement
x : Axis direction
y : Axis direction
z : Axis direction

γ : Unit weight
θ : Axis direction
θ_x : Rotation about x-axis
θ_y : Rotation about y-axis
θ_z : Rotation about z-axis
λ : Critical load factor
ν : Poisson's ratio
ρ : Reinforcement ratio
σ_{cr} : Critical stress
σ_x : Normal stress in x-direction
σ_y : Normal stress in y-direction
τ_{xz} : Transverse shear stress in xz-plane
τ_{yz} : Transverse shear stress in yz-plane
r : Radius
ϕ_{xy} : Shear strain

References

[41.1]: Kárman, Tsien: "*The Buckling of Thin Cylindrical Shells under Axial Compression*"
J. of Aeronatical Science, vol 8, 1941, pp 303-312

[44.1]: A.E.H. Love: "*A Treatise on the Mathematical Theory of Elasticity*"
Dover Publications, New York, 1944

[45.1]: Anker Engelund: "*Brobygning II*"
Jul. Gjellerups Forlag, København, 1945

[61.1]: Timoshenko and Gere:
"*Theory of Elastic Stability*"
McGraw Hill Book Company Inc, New York, 1961

[71.1]: O.C. Zienkiewicz:
"*The Finite Element Method*"
McGraw Hill, London, 1971

[73.1]: W.T. Koiter: "*Elastic Stability, Buckling and Post-buckling Behaviour*"
Report No. 686, Lab. for Eng. Mech., Delft University of Technology, 1980

[79.1]: Jens Kirk: "*Direkte beregning af imperfekte skalkonstruktioner*"
ABK R107, Danmarks Tekniske Højskole, 1979

[88.1]: Phillip L. Gould: "*Analysis of Shells and Plates*"
Springer-Verlag New York Inc, 1988

[92.1]: M. Farshad: "*Design and Analysis of Shell Structures*"
Kluwer, Dordrecht, 1992

[93.1]: J. Christoffersen, L. Jagd, M.P.Nielsen:
"*HOTCH-POTCH Pladeelementet. Finite element til beregning af armerede betonplader*"
ABK R307, Danmarks Tekniske Højskole, 1993

[94.1]: L. Jagd, J. Christoffersen, M.P.Nielsen:
"*The HOTCH-POTCH Disk Element. Finite Element for Analysis of Reinforced Concrete Disks* "
ABK R317, Danmarks Tekniske Universitet, 1994

AFDELINGEN FOR BÆRENDE KONSTRUKTIONER
DANMARKS TEKNISKE UNIVERSITET

Department of Structural Engineering
Technical University of Denmark, DK–2800 Lyngby

SERIE R
(Tidligere: Rapporter)

R 291. JENSEN, HENRIK ELGAARD: Creep and Shrinkage of High–Strength Concrete; A testreport; Appendix B. 1992.
R 292. JENSEN, HENRIK ELGAARD: Creep and Shrinkage of High–Strength Concrete; A testreport; Appendix C. 1992.
R 293. JENSEN, HENRIK ELGAARD: Creep and Shrinkage of High–Strength Concrete; A testreport; Appendix D. 1992.
R 294. JENSEN, HENRIK ELGAARD: Creep and Shrinkage of High–Strength Concrete; An Analysis. 1992.
R 295. JENSEN, HENRIK ELGAARD: State–of–the–art Rapport for Revnet Betons Styrke. 1992.
R 296. IBSØ, JAN BEHRENDT & RASMUSSEN, LARS JUEL: Vridning af armerede normal– og højstyrkebetonbjælker. 1992.
R 297. RIBERHOLT, HILMER, JOHANNESEN, JOHANNES MORSING & RASMUSSEN, LARS JUEL: Rammehjørner med indlimede stålstænger i limtræ. 1992.
R 298. JENSEN, RALPH BO: Modified Finite Element Method modelling Fracture Mechanical Failure in wooden beams. 1992.
R 299. IBSØ, JAN BEHRENDT & AGERSKOV, HENNING: Fatigue Life of Offshore Steel Structures under Stochastic Loading. 1992.
R 300. HANSEN, SVEND OLE: Reliability of Wind Loading on Low–Rise Buildings in a Group. 1992.
R 301. AARRE, TINE: Tensile characteristics of FRC with special emphasis on its applicability in a continuous pavement. 1992.
R 302. GLAVIND, METTE: Evaluation of the Compressive Behaviour of Fiber Reinforced High Strength Concrete. 1992.
R 303. NIELSEN, LEIF OTTO: A C ++ basis for computational mechanics software. 1993
R 304. Resuméoversigt 1992 – Summaries of Papers 1992.
R 305. HANSEN, SØREN, STANG, HENRIK: Eksperimentelt bestemte mekaniske egenskaber for fiberbeton. 1993.
R 306. NIELSEN, PER KASTRUP, ELGAARD JENSEN, HENRIK, SCHMIDT, CLAUS, NIELSEN, M.P.: Forskydning i armerede teglbjælker. 1993.
R 307. CHRISTOFFERSEN, JENS, JAGD, LARS, NIELSEN, M.P.: HOTCHPOTCH Pladeelementet – Finite element til beregning af armerede betonplader. 1993.
R 308. NIELSEN, LEIF OTTO: A C++ class library for FEM special purpose software. 1994.
R 309. DULEVSKI, ENCHO M.: Global Structural Analysis of Steel Box Girder Bridges for Various Loads. 1994.
R 310. Resuméoversigt 1993 – Summaries of Papers 1993.
R 311. JIN–PING ZHANG: Strength of Cracked Concrete. Part 1 – Shear Strength of Conventional Reinforced Concrete Beams, Deep Beams, Corbels, and Prestressed Reinforced Concrete Beams without Shear Reinforcement. 1994.
R 312. OLSEN, DAVID HOLKMANN: Fracture of Concrete A Test Series. 1994.
R 313. OLSEN, DAVID HOLKMANN: Fracture of Concrete A Test Series Appendix I. 1994.
R 314. DAHL, KAARE K.B.: Construction Joints in Normal and High Strength Concrete. 1994.
R 315. KARLSHØJ, JAN: Principper og metoder for opstilling af datamodeller til byggetekniske anvendelser. 1994.

Abonnement 1.7.1993 – 30.6.1994 kr. 130,–
Subscription rate 1.7.1993 – 30.6.1994 D.Kr. 130.–.

Hvis De ikke allerede modtager Afdelingens resuméoversigt ved udgivelsen, kan Afdelingen tilbyde at tilsende næste års resuméoversigt, når den udgives, dersom De udfylder og returnerer nedenstående kupon.

Returneres til
Afdelingen for Bærende Konstruktioner
Danmarks Tekniske Universitet
Bygning 118
2800 Lyngby

Fremtidig tilsendelse af resuméoversigter udbedes af
(bedes udfyldt med blokbogstaver):
Stilling og navn: .....
Adresse: .....
Postnr. og -distrikt: .....

The Department has pleasure in offering to send you a next year's list of summaries, free of charge. If you do not already receive it upon publication, kindly complete and return the coupon below.

To be returned to:
Department of Structural Engineering
Technical University of Denmark
Building 118
DK-2800 Lyngby, Denmark.

The undersigned wishes to receive the Department's List of Summaries:
(Please complete in block letters)
Title and name: .....
Address: .....
Postal No. and district: .....
Country: .....